Résolution de l'ETR par une méthode de volumes finis modifiés – application à la détection de tumeurs cancéreuses

Fatmir Asllanaj[1], CR CNRS HDR

Sylvain Contassot-Vivier[2], Ahmad Addoum[1], Olivier Farges[1]

[1]LEMTA, [2]LORIA

SFT, 22 Novembre 2017

Outline

- Introduction
- The **M**odified **F**inite **V**olume **M**ethod
- The reconstruction algorithm and results
  - with diffuse light
  - with fluorescence light
- Conclusions, future works

Motivation

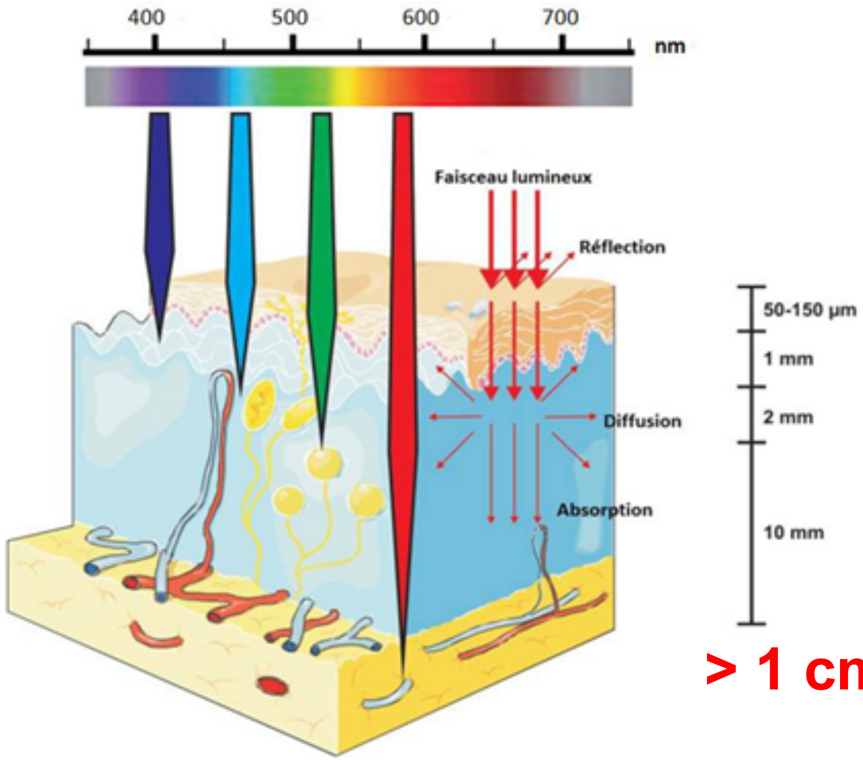

> 1 cm

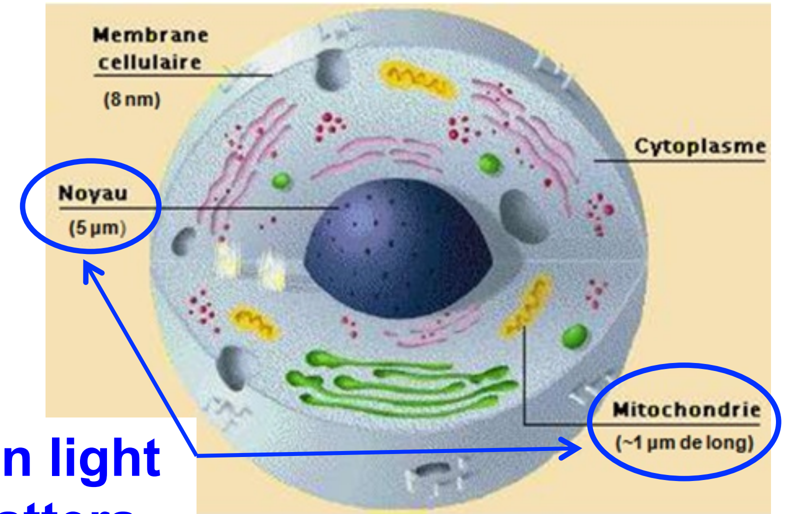

Main light scatters

also membranes (lipids) and collagene fibers

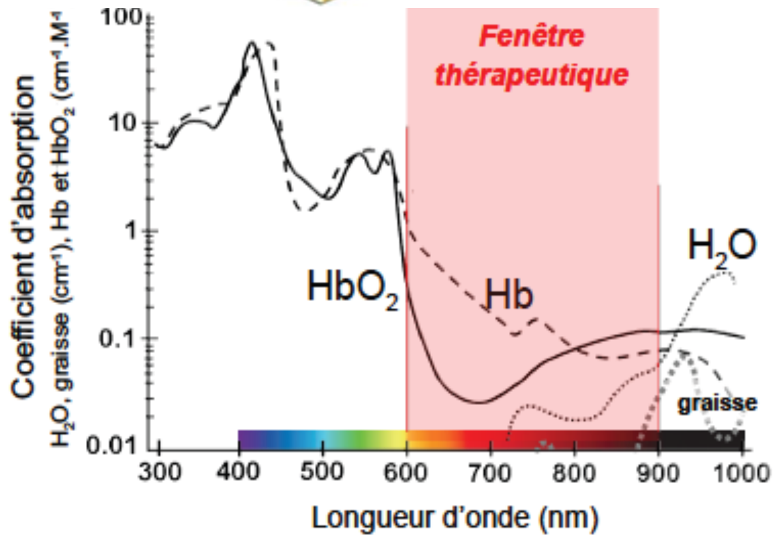

Skin has a complex structure

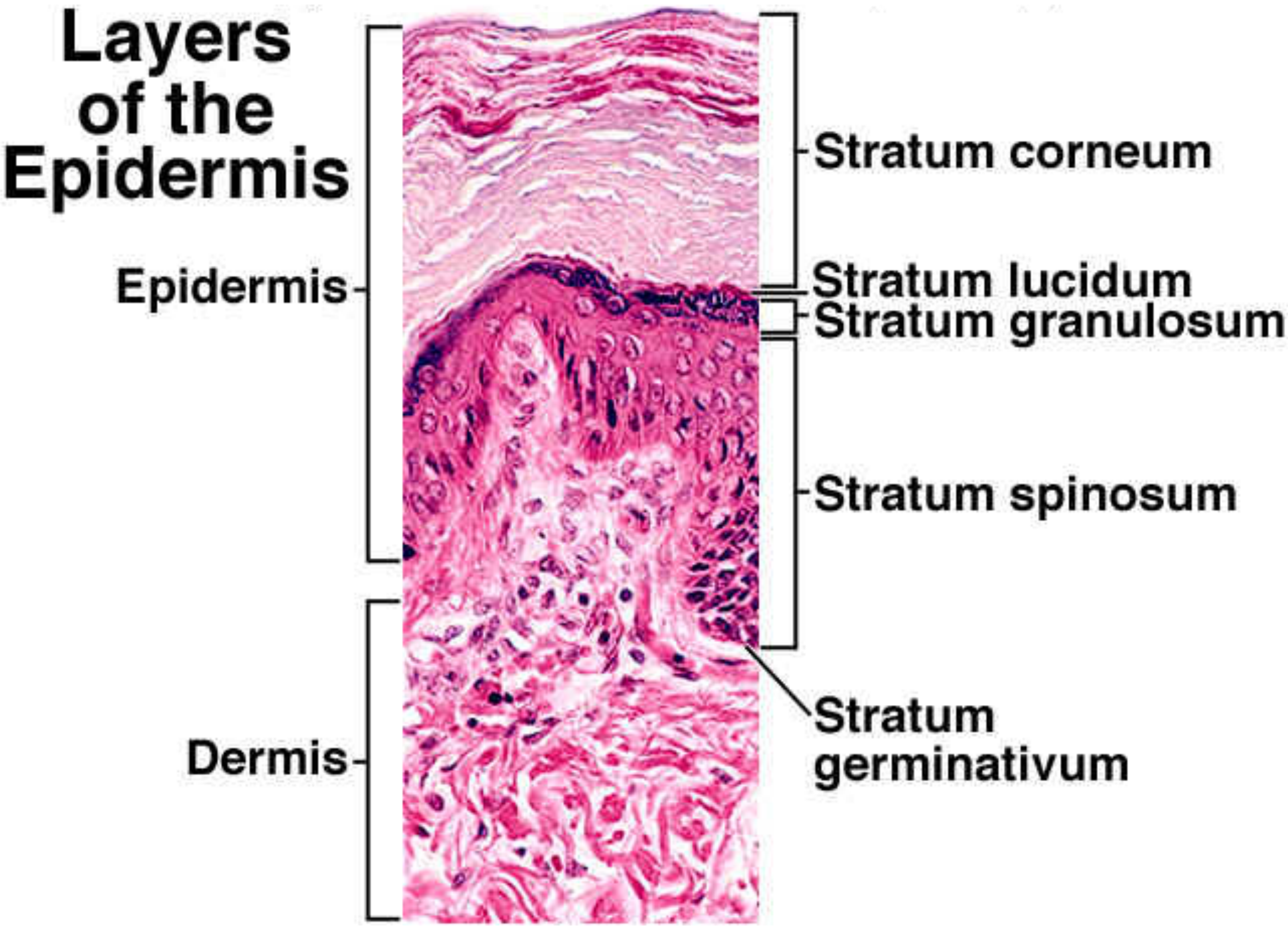

How a cancer tumor can be detected?

- The cancer leads to physiological changes that affect the optical properties (scattering, absorption, asymmetry factor,…) of biological tissues
- A tumor is highly vascularized: **change** in **absorption** coefficients
- Change in size of nucleus of cancer cells: **change** in **scattering** coefficients

	Healthy liver	Metastatic liver
Absorption coefficient μ_a (mm^{-1})	0.1	0.06
Scattering coefficient μ_s (mm^{-1})	20.4	10.8
Asymmetry factor g	0.955	0.902
Optical penetration depth (mm)	1.8	2.3

Germer et al., Laser Sureg Med, 1998

Different methods for solving the RTE

Diffusion Equation → Restrictive assumptions

Statistical method, Monte Carlo
(accurate, complex geometries, fast with GPU/MPI)
Inverse MC: difficult convergence

Deterministic methods
(PDE)

Analytical solutions (accurate, very fast, simple cases)

Numerical solutions

" **false scattering** " (spatial discretization)
"**ray-effect** " (angular discretization)

Angular discretization

- Discrete direction $\mathbf{\Omega}^{\mathbf{k}}$ with an azimutal angle $\theta \in [0, 2\pi]$ and a polar angle $\varphi \in [0, \pi]$

- Constant step

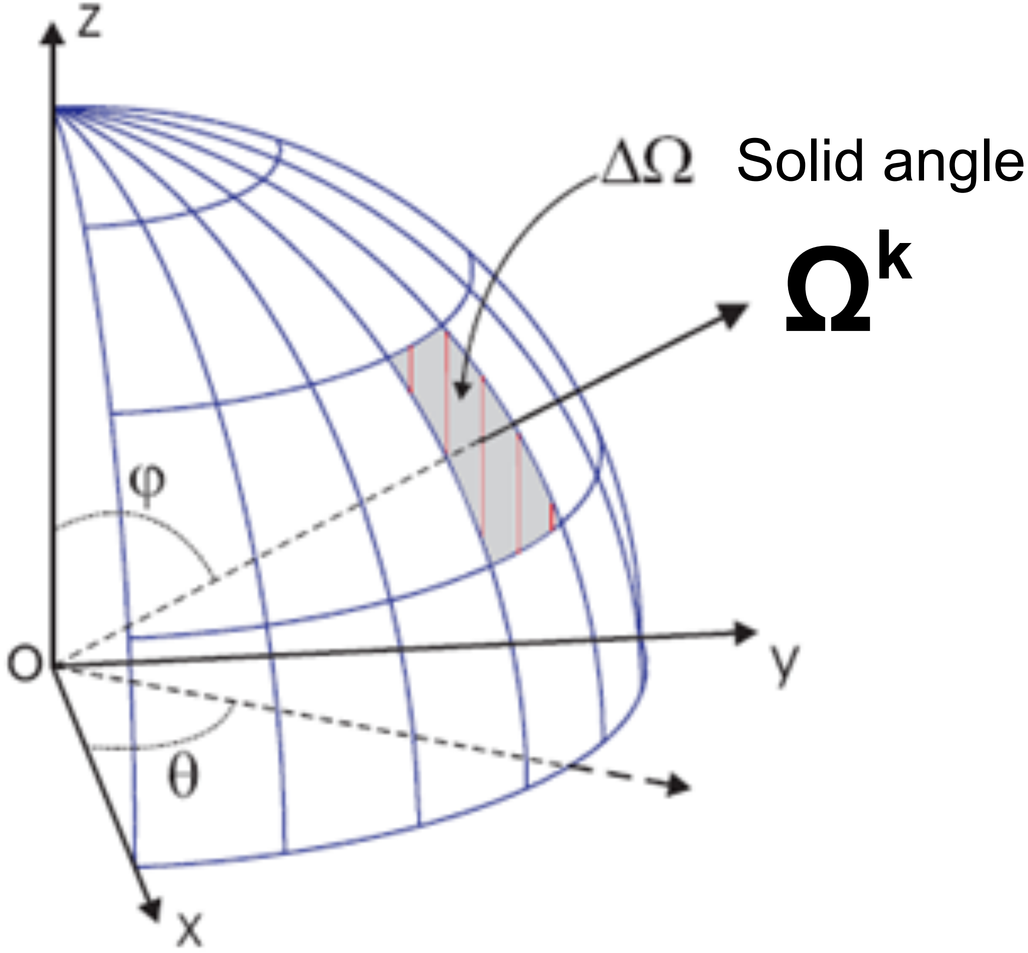

Applying the angular discretization to the RTE

$$\frac{n_\lambda(s)}{c}\frac{\partial \psi_\lambda(s,\mathbf{\Omega^k},t)}{\partial t} + \mathbf{\Omega^k}\cdot\nabla\psi_\lambda(s,\mathbf{\Omega^k},t) = -\mu_{t\lambda}(s)\,\psi_\lambda(s,\mathbf{\Omega^k},t)$$

$$+\,\mu_{s\lambda}(s)\sum_{k'=1}^{N} p_\lambda(\mathbf{\Omega^{k'}},\mathbf{\Omega^k})\,\psi_\lambda(s,\mathbf{\Omega^{k'}},t)\,\omega^{k'} + S_\lambda(s,\mathbf{\Omega^k},t)$$

Applying the angular discretization to the RTE

$$\frac{n_\lambda(s)}{c}\frac{\partial \psi_\lambda(s,\mathbf{\Omega}^{\mathbf{k}},t)}{\partial t} + \mathbf{\Omega}^{\mathbf{k}} \cdot \nabla \psi_\lambda(s,\mathbf{\Omega}^{\mathbf{k}},t) = -\mu_{t\lambda}(s)\psi_\lambda(s,\mathbf{\Omega}^{\mathbf{k}},t)$$

$$+\mu_{s\lambda}(s)\sum_{k'=1}^{N} p_\lambda(\mathbf{\Omega}^{\mathbf{k'}},\mathbf{\Omega}^{\mathbf{k}})\psi_\lambda(s,\mathbf{\Omega}^{\mathbf{k'}},t)\,\omega^{k'} + S_\lambda(s,\mathbf{\Omega}^{\mathbf{k}},t)$$

- First, the simplified equation (steady-state, wavelength indepedent properties, non-scattering) has to be solved:

$$\mathbf{\Omega}^{\mathbf{k}} \cdot \nabla \psi(s,\mathbf{\Omega}^{\mathbf{k}}) = -\mu_a(s)\psi(s,\mathbf{\Omega}^{\mathbf{k}}) + S(s,\mathbf{\Omega}^{\mathbf{k}})$$

- The sum with scattering and BC are taken into account by iterations

Applying the angular discretization to the RTE

$$\frac{n_\lambda(s)}{c}\frac{\partial \psi_\lambda(s,\mathbf{\Omega^k},t)}{\partial t} + \mathbf{\Omega^k}\cdot\nabla\psi_\lambda(s,\mathbf{\Omega^k},t) = -\mu_{t\lambda}(s)\,\psi_\lambda(s,\mathbf{\Omega^k},t)$$

$$+\,\mu_{s\lambda}(s)\sum_{k'=1}^{N} p_\lambda(\mathbf{\Omega^{k'}},\mathbf{\Omega^k})\,\psi_\lambda(s,\mathbf{\Omega^{k'}},t)\,\omega^{k'} + S_\lambda(s,\mathbf{\Omega^k},t)$$

- First, the simplified equation (steady-state, wavelength indepedent properties, non-scattering) has to be solved:

$$\mathbf{\Omega^k}\cdot\nabla\psi(s,\mathbf{\Omega^k}) = -\mu_a(s)\,\psi(s,\mathbf{\Omega^k}) + S(s,\mathbf{\Omega^k})$$

- The sum with scattering and BC are taken into account by iterations
- The normalization technique is applied to the H-G phase function:

$$\tilde{p}^{m\to n} = \frac{\int_{\Delta\Omega^m}\int_{\Delta\Omega^n} p(\mathbf{\Omega'}\cdot\mathbf{\Omega})\,d\Omega'\,d\Omega}{\Delta\Omega^m\,\Delta\Omega^n} \qquad p(\mathbf{\Omega'}\cdot\mathbf{\Omega}) = \frac{1}{4\pi}\frac{1-g^2}{(1+g^2-2g\,\mathbf{\Omega'}\cdot\mathbf{\Omega})^{3/2}}$$

2D control volume with a cell-vertex formulation

- The RTE has to be solved at **each node of the mesh**

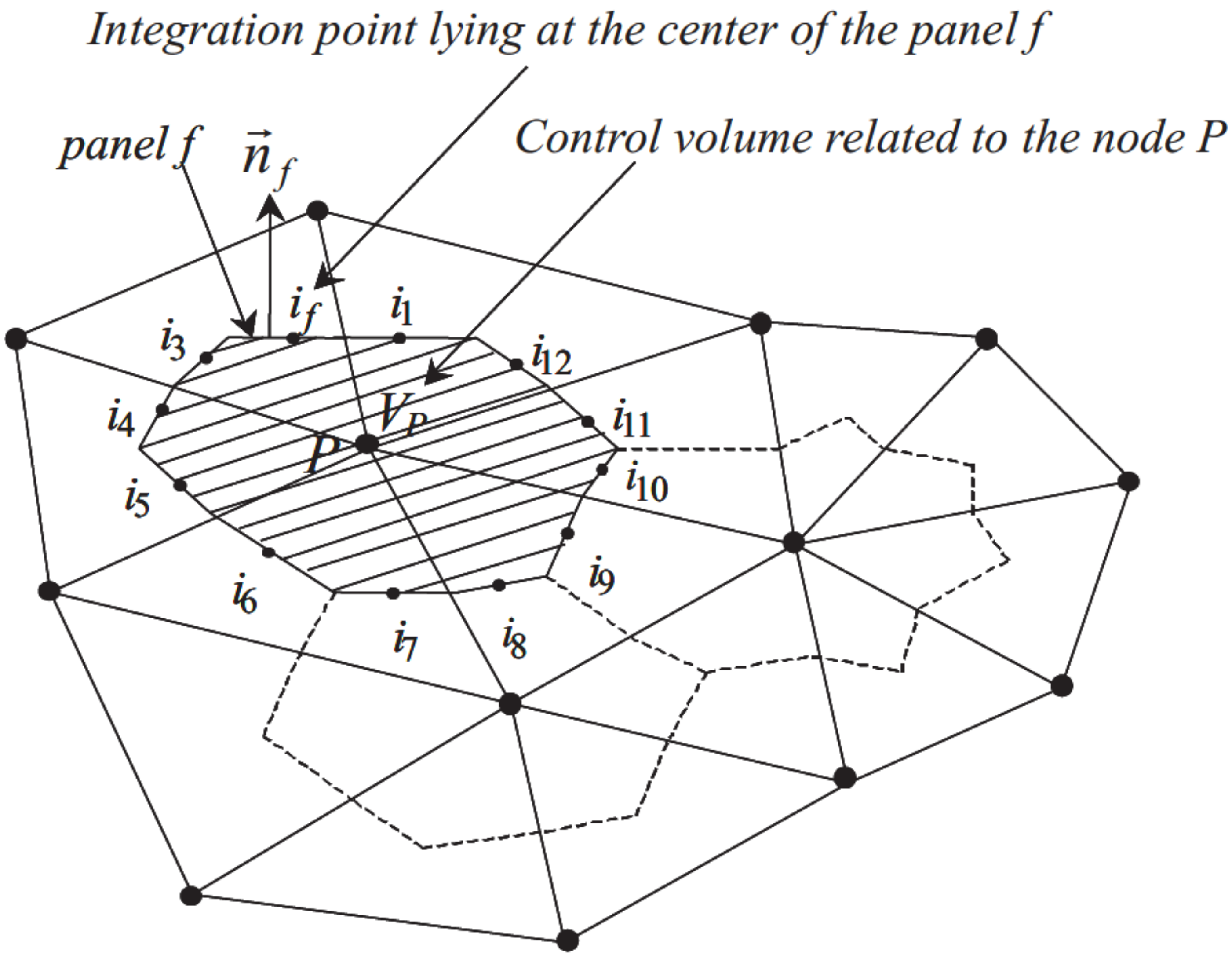

(Classical) FVM applied to the RTE

Applying Gauss divergence theorem:

$$\int_{\Gamma_P}\int_{\Delta\Omega^k} \psi(s,\mathbf{\Omega})\,(\mathbf{\Omega}\cdot\mathbf{n}_{\mathbf{out}})\,d\Omega\,dS = \int_{V_P}\int_{\Delta\Omega^k} -\mu_a(s)\,\psi(s,\mathbf{\Omega}) + S(s,\mathbf{\Omega})\,d\Omega\,dV$$

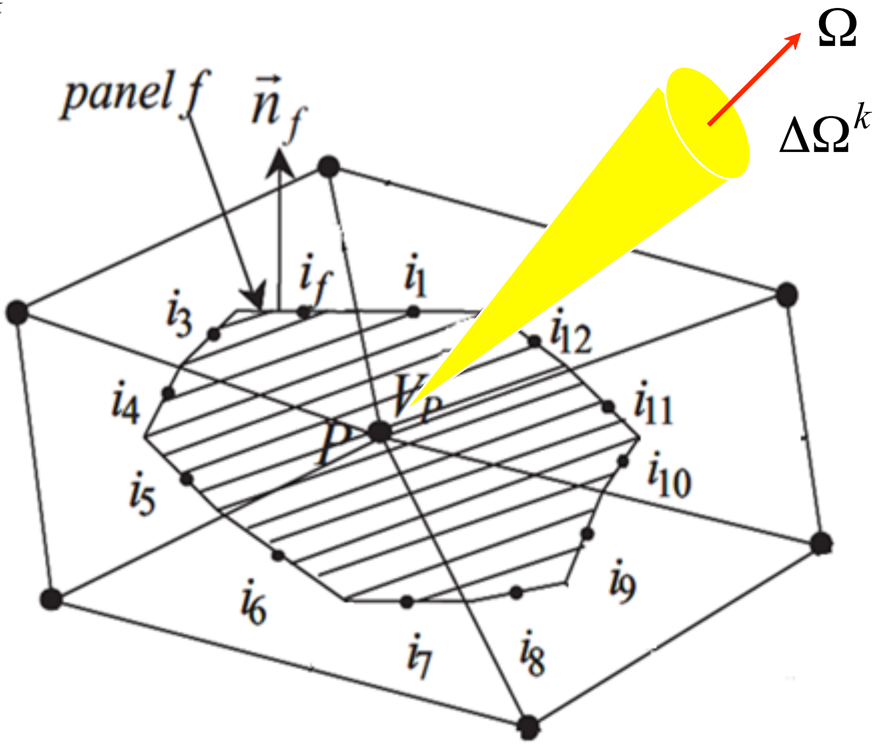

- If one considers:

  - an average value ψ_P^k in V_P
  - an average value $\psi_{i_f}^k$ on a panel *f*

  A_f is the length of the panel *f*

$$\Delta_f^k = \int_{\Delta\Omega^k} (\mathbf{\Omega}\cdot\mathbf{n}_f)\ d\Omega$$

- The FVM gives: $$\sum_{f=1}^{N_f} \psi_{i_f}^k\ A_f\ \Delta_f^k = \left[-\mu_{a,P}\,\psi_P^k + S_P^k\right]\Delta\Omega^k\ V_P$$

Conservation of energy

(Classical) FVM applied to the RTE

Applying Gauss divergence theorem:

$$\int_{\Gamma_P}\int_{\Delta\Omega^k} \psi(s,\mathbf{\Omega})\,(\mathbf{\Omega}\cdot\mathbf{n}_{\mathrm{out}})\,d\Omega\,dS = \int_{V_P}\int_{\Delta\Omega^k} -\mu_a(s)\,\psi(s,\mathbf{\Omega}) + S(s,\mathbf{\Omega})\,d\Omega\,dV$$

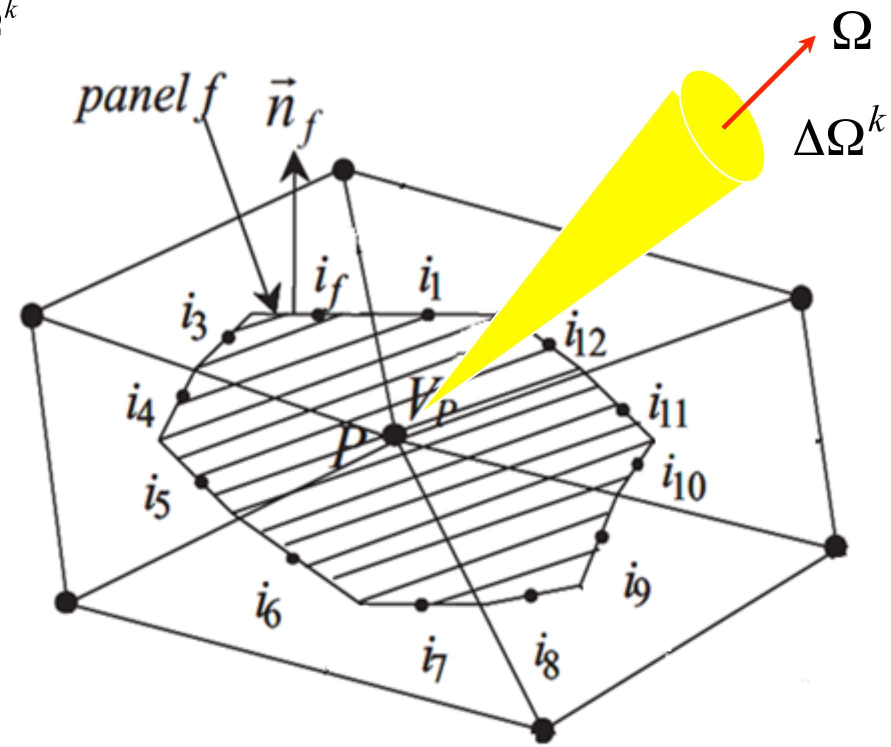

- If one considers:

 - an average value ψ_P^k in V_P

 - an average value $\psi_{i_f}^k$ on a panel *f*

 A_f is the length of the panel *f*

$$\Delta_f^k = \int_{\Delta\Omega^k} (\mathbf{\Omega}\cdot\mathbf{n}_f)\;d\Omega$$

?

- The FVM gives: $\displaystyle\sum_{f=1}^{N_f} \psi_{i_f}^k\; A_f\,\Delta_f^k = \left[-\mu_{a,P}\,\psi_P^k + S_P^k\right]\Delta\Omega^k\,V_P$

Exponential scheme for the closure relations

- Integral form of the RTE

$$\psi_{i_f}^k = \psi_{u_f}^k \exp\left(-\int_{u_f}^{i_f} \mu_a(s)\, ds\right) + \int_{u_f}^{i_f} S^k(s) \exp\left(-\int_{s}^{i_f} \mu_a(u)\, du\right) ds$$

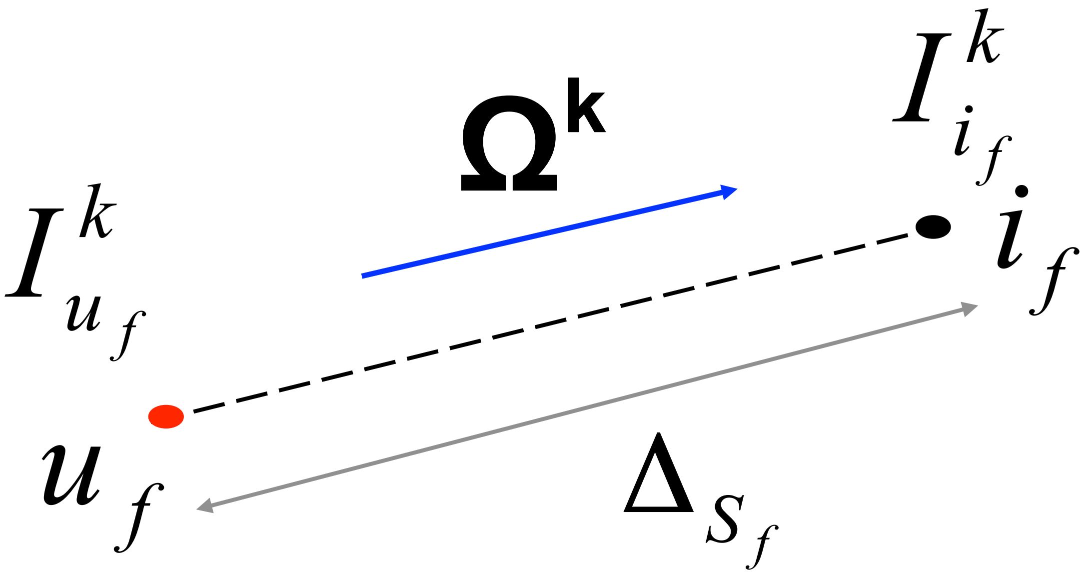

- $\psi_{u_f}^k$ has to be determined according to the radiances given at the nodes of the mesh

2D projections and interpolations

- for a reference triangle

$$\psi_{u_1}^{k} \cong \psi_{P_1}^{k}$$

$$\psi_{u_2}^{k} \cong \psi_{P_1}^{k}$$

$$\psi_{u_3}^{k} \cong \frac{|u_3\, P_2|}{|P_1\, u_3| + |u_3\, P_2|}\psi_{P_1}^{k} + \frac{|P_1\, u_3|}{|P_1\, u_3| + |u_3\, P_2|}\psi_{P_2}^{k}$$

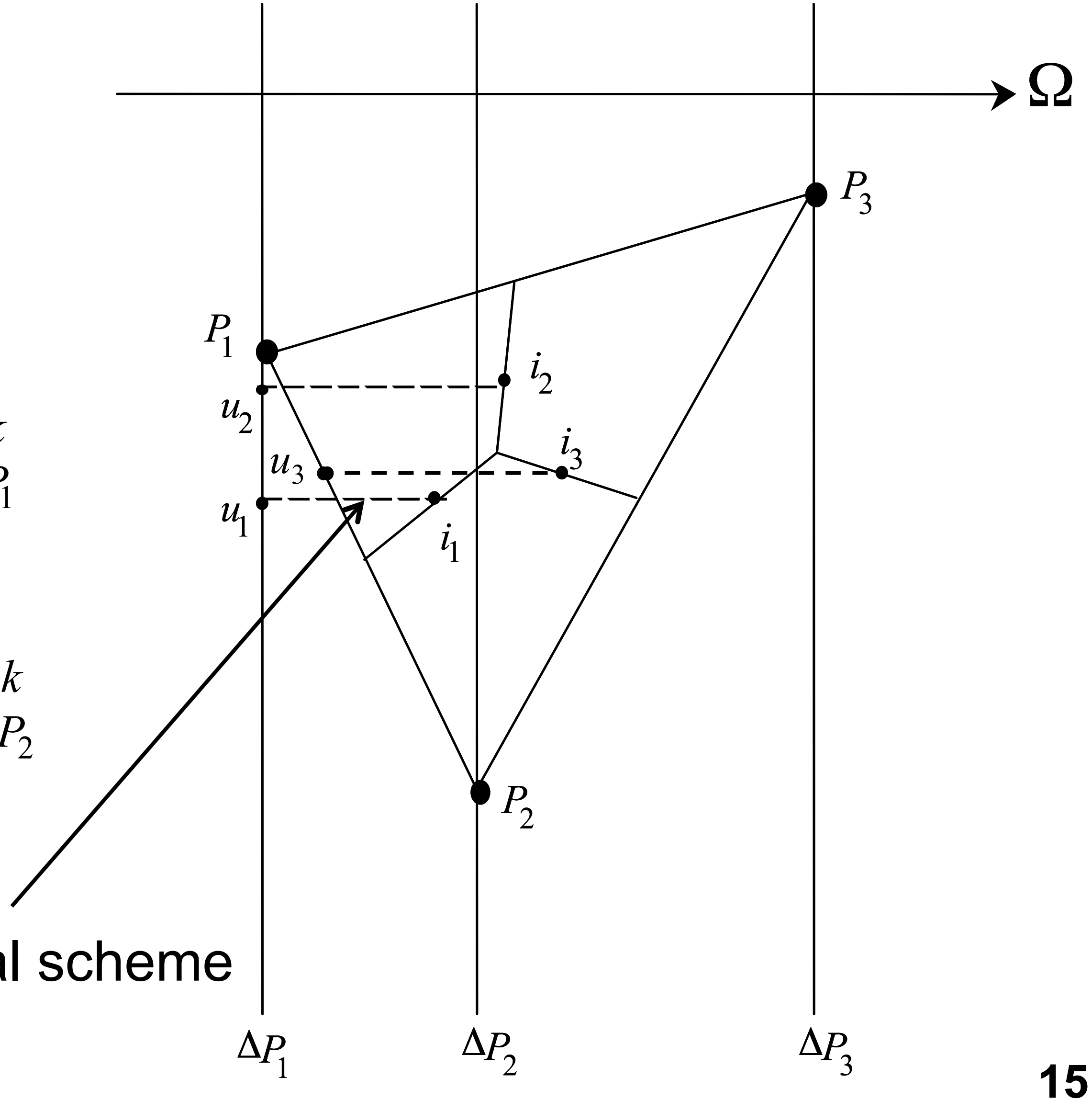

Solution for the radiative intensity

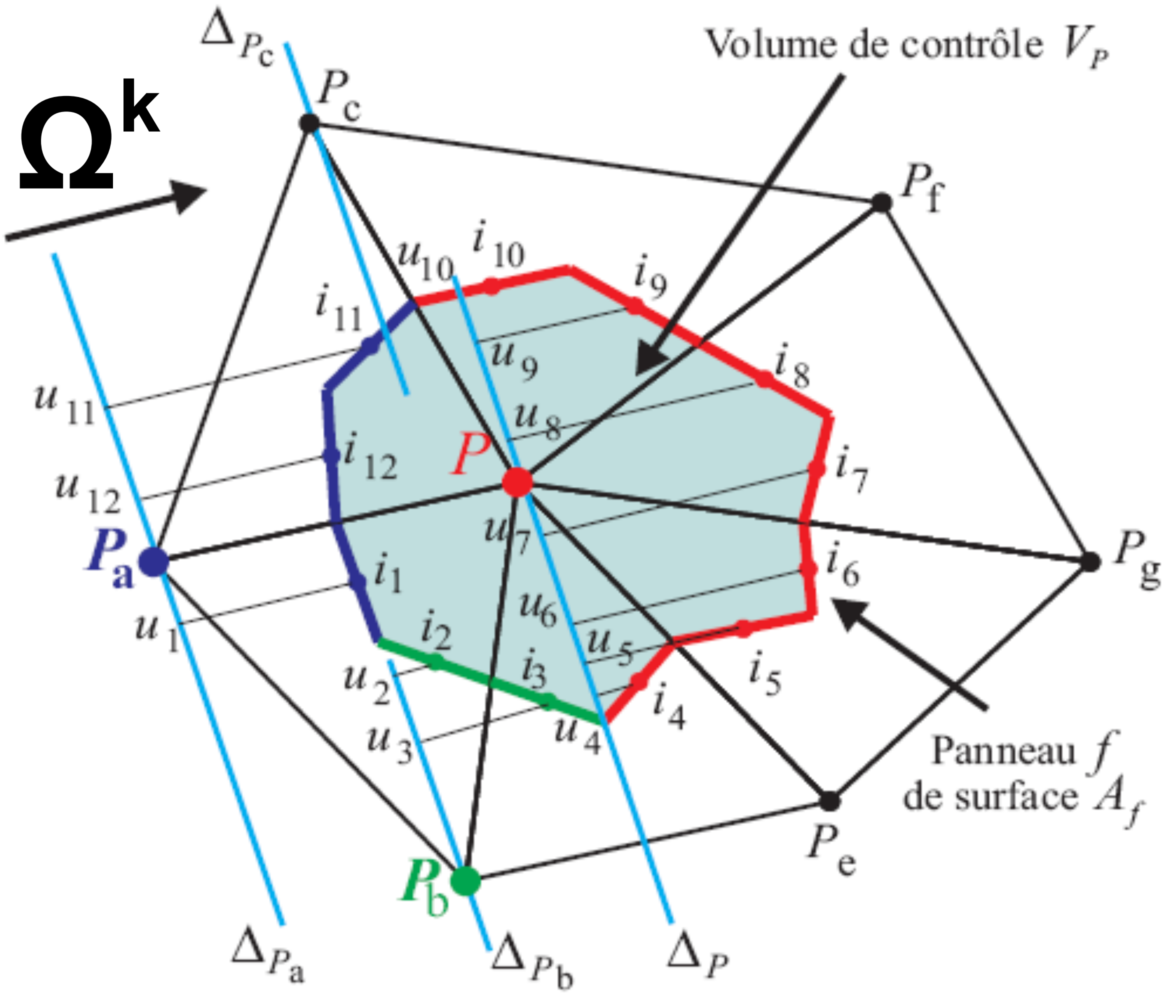

Explicit solution: $I_P^k = f(I_{P_a}^k, I_{P_b}^k, I_{P_c}^k)$

Marching order map

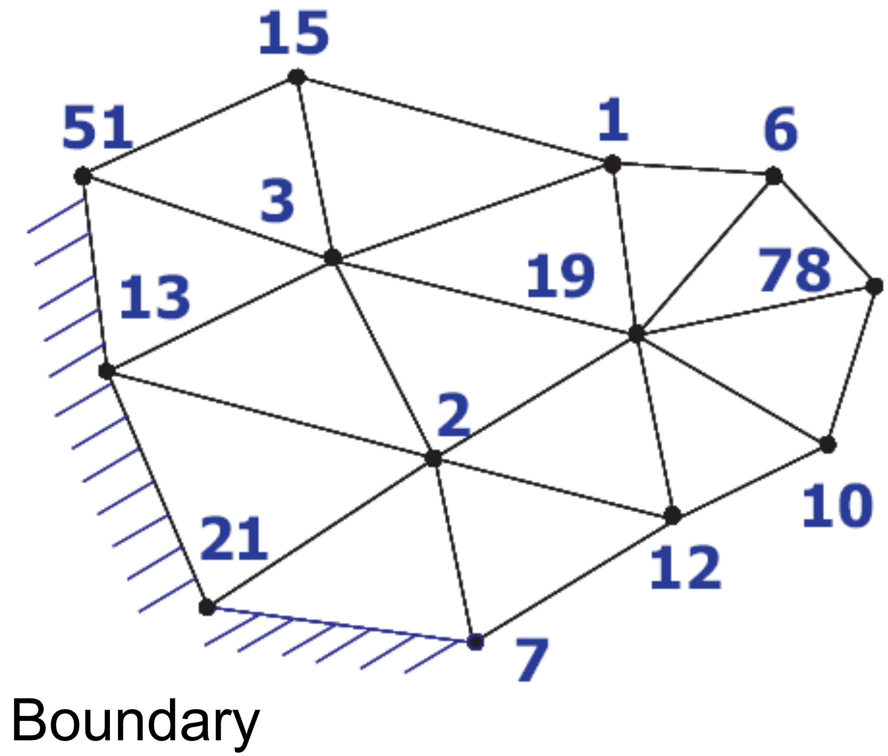

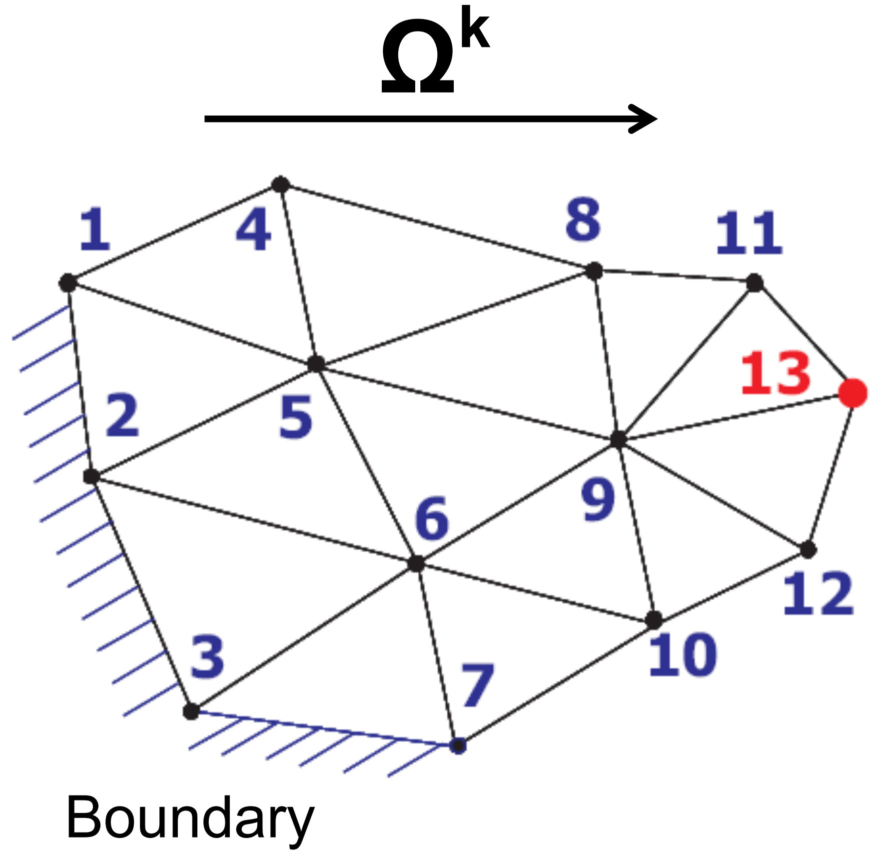

Initial mesh

Renumbered mesh according to the given direction

3D control volume

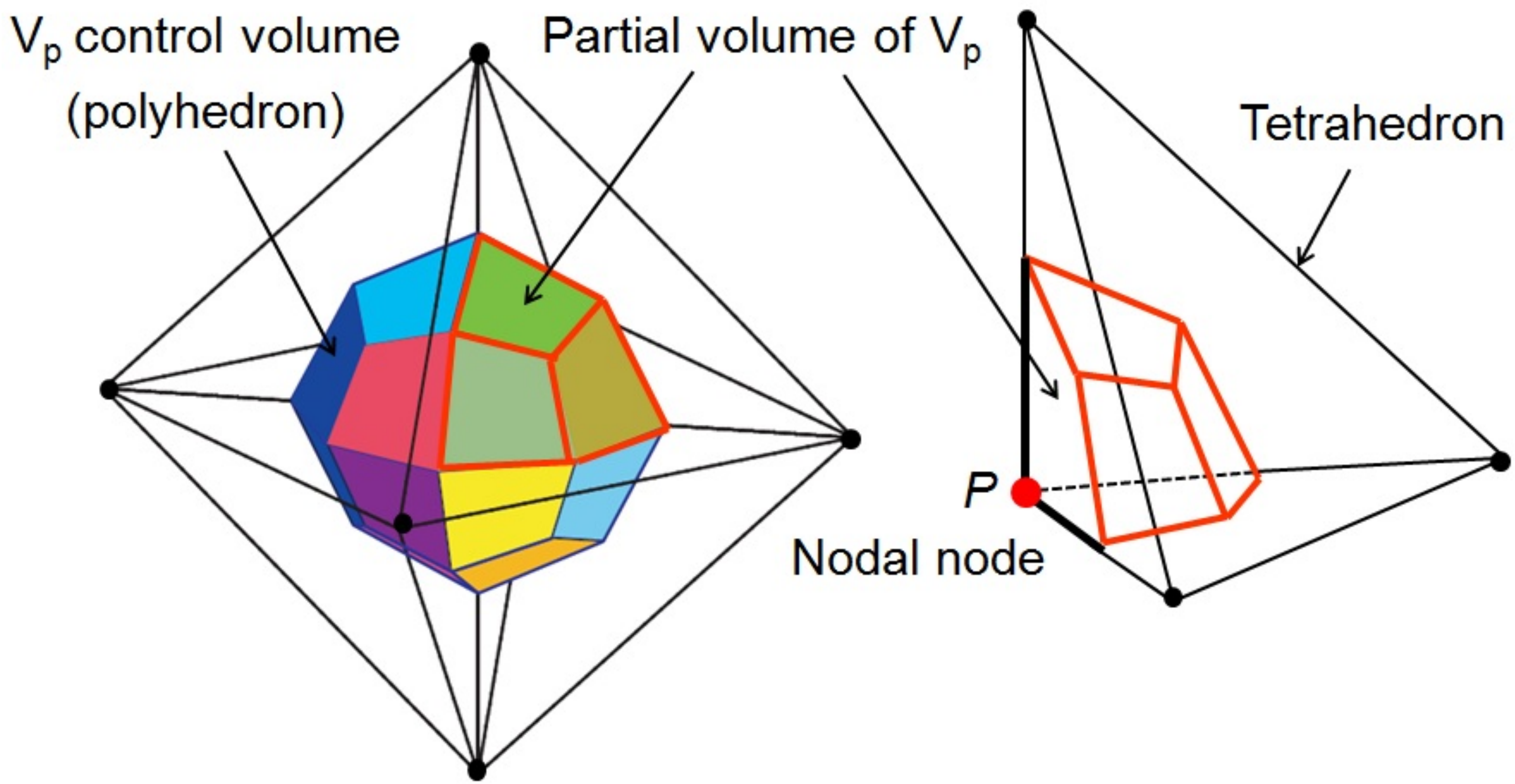

3D projections and interpolations

- for a reference tetrahedron

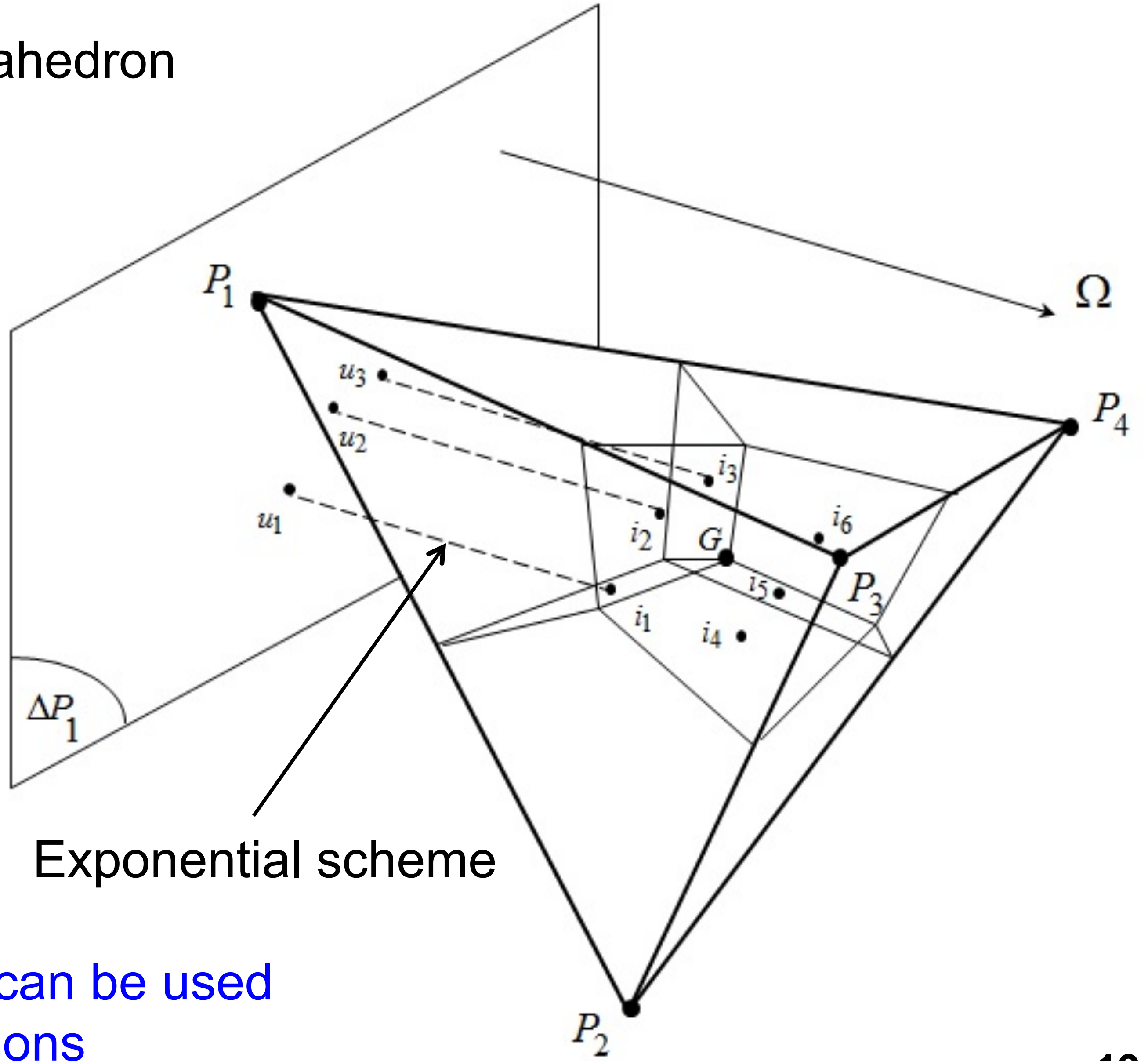

Up to **3** nodal nodes can be used for interpolations

Validation of the 2D/3D MFVM

- **Relative differences < 1%** on the reflectances or transmittances with a suitable mesh (**comparison with MC or "analytical solutions"**)

Conditions: homogeneous and two layered media,
semi-transparent boundaries (with Fresnel reflections at the interface),
steady-state and time domains

Asllanaj et al. (**2014**), **J Biomedical Optics**

Asllanaj et al. ***Fluorescence*** *and diffuse light propagation in biological tissue based on the 3D radiative transport equation. Part I: computational method*

Asllanaj et al*. Part II: simulations*

Asllanaj and Fumeron (**2012**), **J Biomedical Optics**

Asllanaj et al. (**2015**), ***JQSRT***

The RTE in the frequency domain

$$\underbrace{\frac{i\omega}{c/n}\psi(\boldsymbol{r},\boldsymbol{\Omega},\omega)}_{\text{Frequential variations}} + \underbrace{\boldsymbol{\Omega}\cdot\nabla\psi(\boldsymbol{r},\boldsymbol{\Omega},\omega)}_{\text{Spatial variations}} = \underbrace{-(\mu_s(\boldsymbol{r})+\mu_a(\boldsymbol{r}))\psi(\boldsymbol{r},\boldsymbol{\Omega},\omega)}_{\text{Loss by extinction}}$$

$$+ \underbrace{\mu_s(\boldsymbol{r})\int_{\Omega'=4\pi} p(\boldsymbol{\Omega'},\boldsymbol{\Omega})\,\psi(\boldsymbol{r},\boldsymbol{\Omega'},\omega)\,d\Omega'}_{\text{Reinforcement by scattering}} + \underbrace{S(\boldsymbol{r},\boldsymbol{\Omega},\omega)}_{\text{Source term}}$$

- refractive index $n\,(=1.4)$
- absorption and scattering coefficients $\mu_s,\ \mu_a$
- asymmetry factor (Henyey-Greenstein) g

• Henyey-Greenstein (H-G): $p(\boldsymbol{\Omega'}\cdot\boldsymbol{\Omega}) = \dfrac{1}{4\pi}\dfrac{1-g^2}{(1+g^2-2g\,\boldsymbol{\Omega'}\cdot\boldsymbol{\Omega})^{3/2}}$

The RTE in the frequency domain

$$\underbrace{\frac{i\omega}{c/n}\psi(\boldsymbol{r},\boldsymbol{\Omega},\omega)}_{\text{Frequential variations}} + \underbrace{\boldsymbol{\Omega}\cdot\nabla\psi(\boldsymbol{r},\boldsymbol{\Omega},\omega)}_{\text{Spatial variations}} = \underbrace{-(\mu_s(\boldsymbol{r})+\mu_a(\boldsymbol{r}))\psi(\boldsymbol{r},\boldsymbol{\Omega},\omega)}_{\text{Loss by extinction}}$$

$$+ \underbrace{\mu_s(\boldsymbol{r})\int_{\Omega'=4\pi} p(\boldsymbol{\Omega}',\boldsymbol{\Omega})\,\psi(\boldsymbol{r},\boldsymbol{\Omega}',\omega)\,d\Omega'}_{\text{Reinforcement by scattering}} + \underbrace{S(\boldsymbol{r},\boldsymbol{\Omega},\omega)}_{\text{Source term}}$$

- refractive index $n\,(=1.4)$
- absorption and scattering coefficients μ_s, μ_a
- asymmetry factor (Henyey-Greenstein) g

the most sensitive parameter *

- reduced scattering coefficient $(=\mu_s(1-g))$ μ_s'

coefficients usually estimed or reconstructed

*Marin, Asllanaj, Maillet (**2014**), **JQSRT**

Reconstruction of the optical properties

- PhD thesis of Ahmad Addoum (2014 - 2017)
- From boundary data (reflectance)

$$J(\theta) = \frac{1}{2}\left\| R(\theta) - d_{obs} \right\|^2$$

Reconstruction of the optical properties

- PhD thesis of Ahmad Addoum (2014 - 2017)
- From boundary data (reflectance)

$$J(\theta) = \frac{1}{2}\left\| R(\theta) - d_{obs} \right\|^2$$

- The reconstruction algorithm is based on an iterative solution of the RTE (forward model) and his adjoint state (solved also with the MVFM)

$$\frac{-i\omega}{c/n}\phi(\boldsymbol{r},\boldsymbol{\Omega},\omega) - \boldsymbol{\Omega}\cdot\nabla\phi(\boldsymbol{r},\boldsymbol{\Omega},\omega) = -(\mu_s(\boldsymbol{r}) + \mu_a(\boldsymbol{r}))\,\phi(\boldsymbol{r},\boldsymbol{\Omega},\omega)$$

$$+\,\mu_s(\boldsymbol{r})\int_{\Omega'=4\pi} p(\boldsymbol{\Omega}',\boldsymbol{\Omega})\,\phi(\boldsymbol{r},\boldsymbol{\Omega}',\omega)\,d\Omega' + \underbrace{H(\boldsymbol{r},\boldsymbol{\Omega},\omega)}_{\text{Adjoint source term}}$$

- Update reconstructed parameters with Lm-BFGS using an efficient calculation of $\nabla J(\theta)$

2D reconstruction of the optical properties

4 illuminated boundaries, 10 frequencies on [100 MHz; 1 GHz]

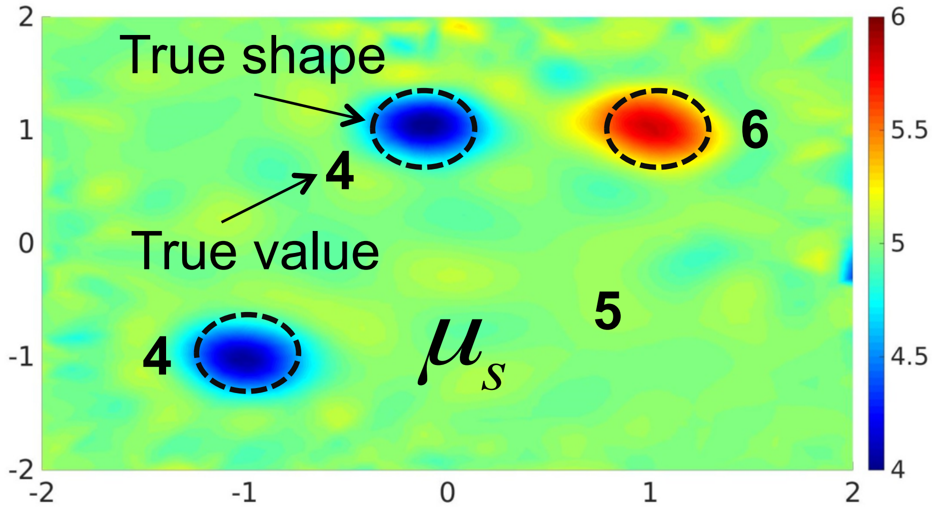

Outside the inclusions:

$$\mu_s = 5\ \mathrm{mm}^{-1}$$

$$\mu_a = 0.05\ \mathrm{mm}^{-1}$$

$$g = 0.9$$

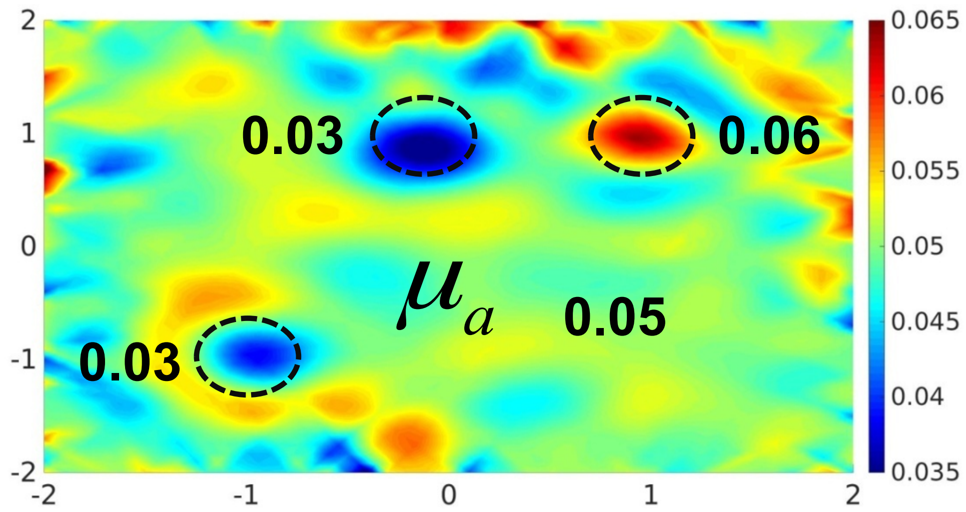

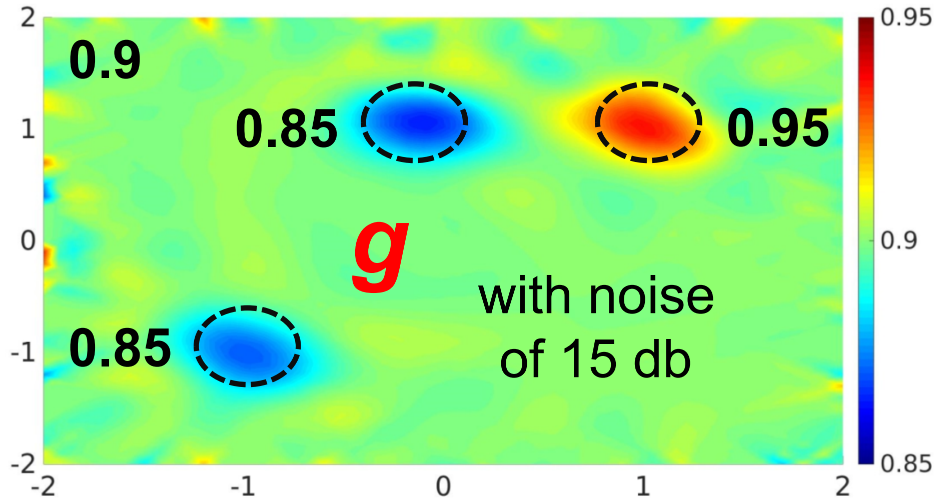

Reconstruction of μs for skin

Top boundary illuminated $\mu_a = 0.05\ \mathrm{mm}^{-1}, g = 0.8$

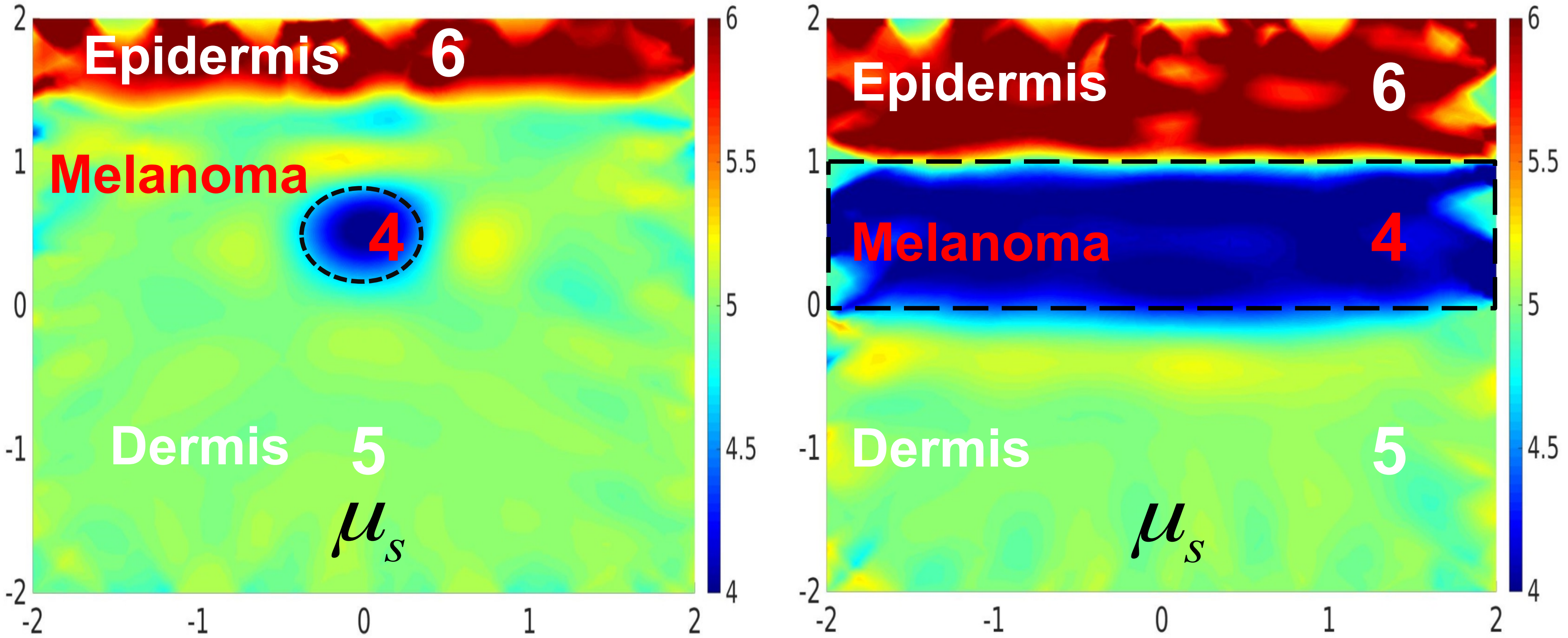

Addoum et al. (**2018**), **JQSRT**

3D reconstruction

$\mu_s = 4\ \text{mm}^{-1}$

C = (1,1,1)

D = 1 mm

Gaussian beam

Pulse width :

0.5 mm

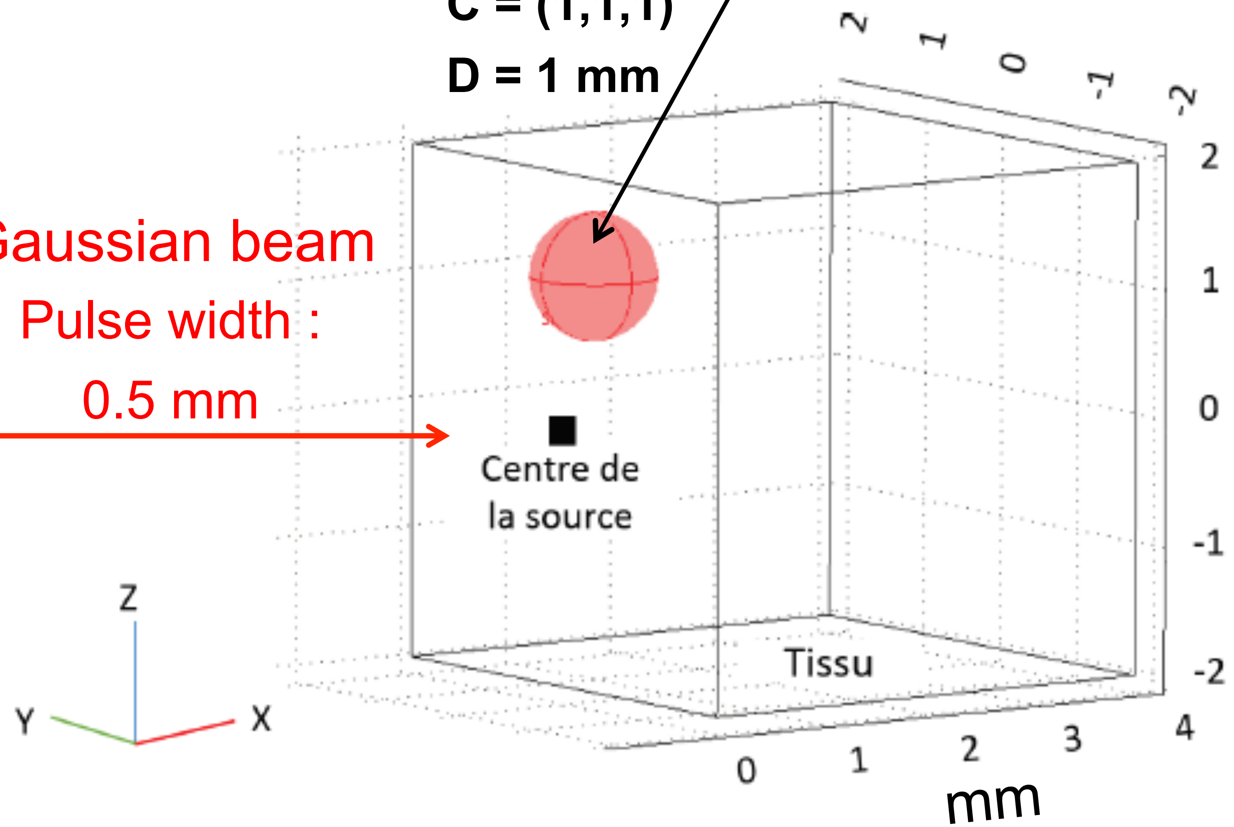

Outside the inclusion:

$\mu_a = 0.01\ \text{mm}^{-1}$

$\mu_s = 2\ \text{mm}^{-1}$

$g = 0.8$

100 000 nodes (spatial mesh), 64 directions

(simulated boundary data obtained with this mesh)

Reconstruction of μs

600 MHz

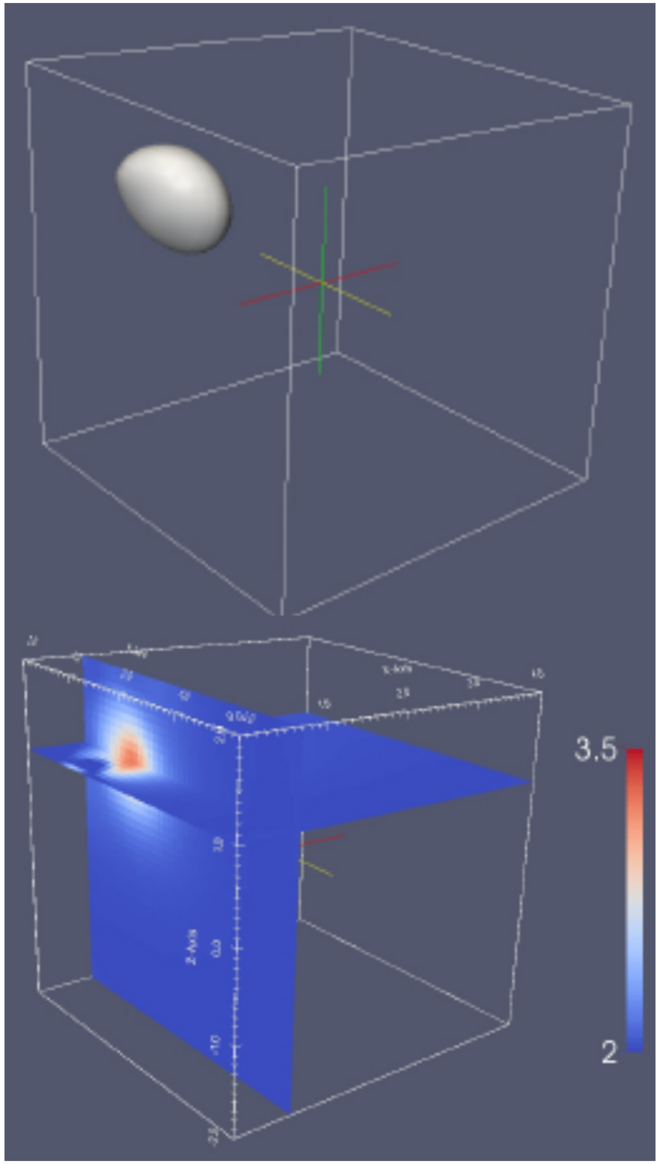

5 frequencies in [100 MHz, 1 GHz]

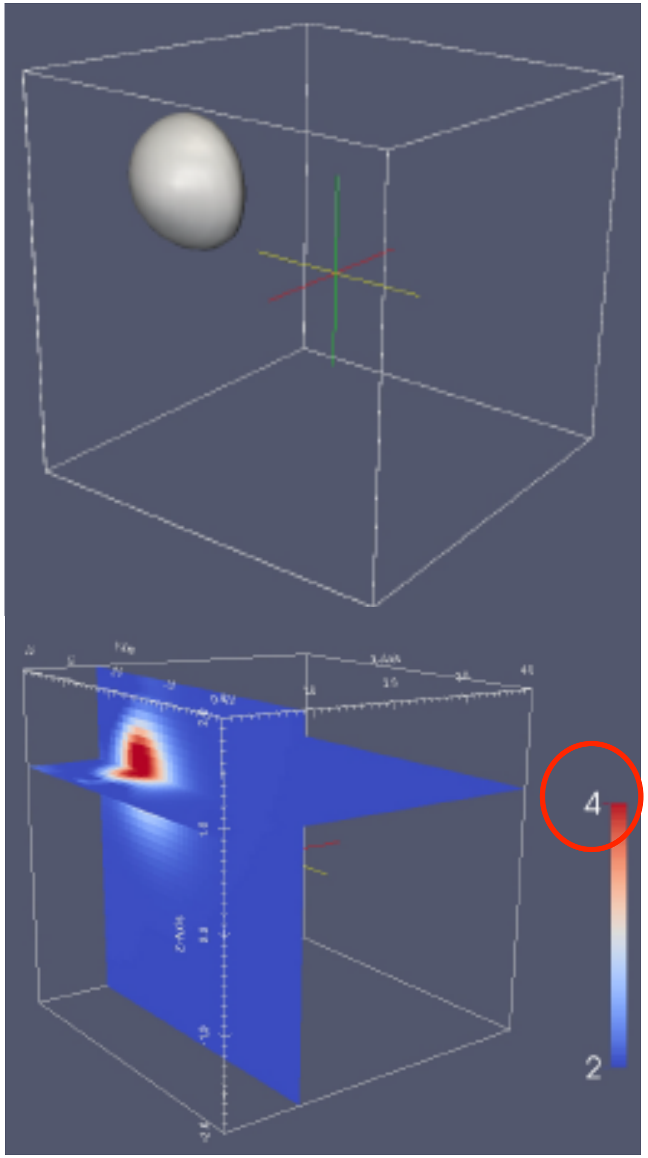

Reconstruction of μs

600 MHz

$\mu_s = 4\ \text{mm}^{-1}$

L = 4 mm

D = 1 mm

depth = 1 mm

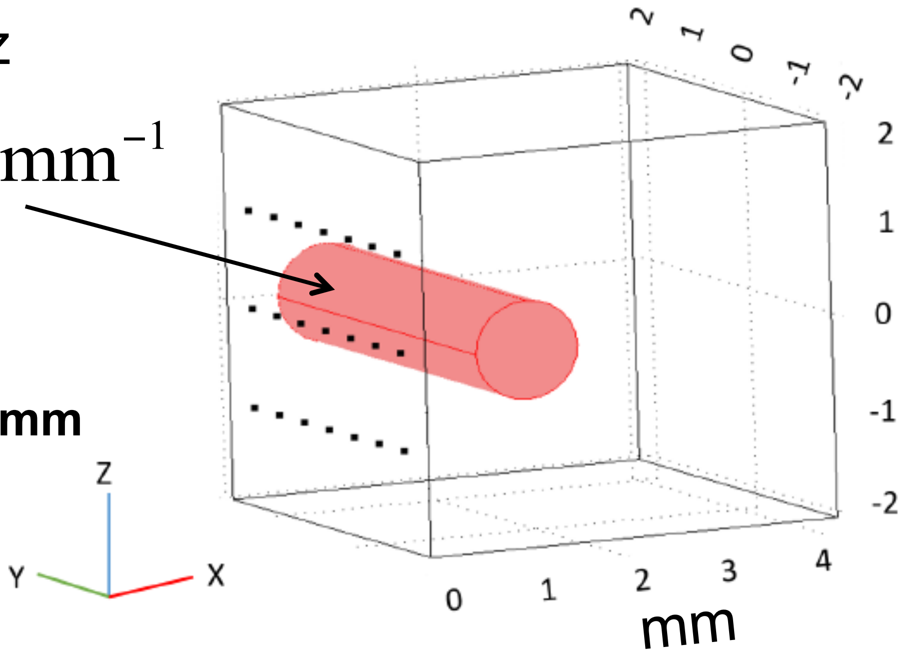

Outside the inclusion:

$\mu_a = 0.01\ \text{mm}^{-1}$

$\mu_s = 2\ \text{mm}^{-1}$

$g = 0.8$

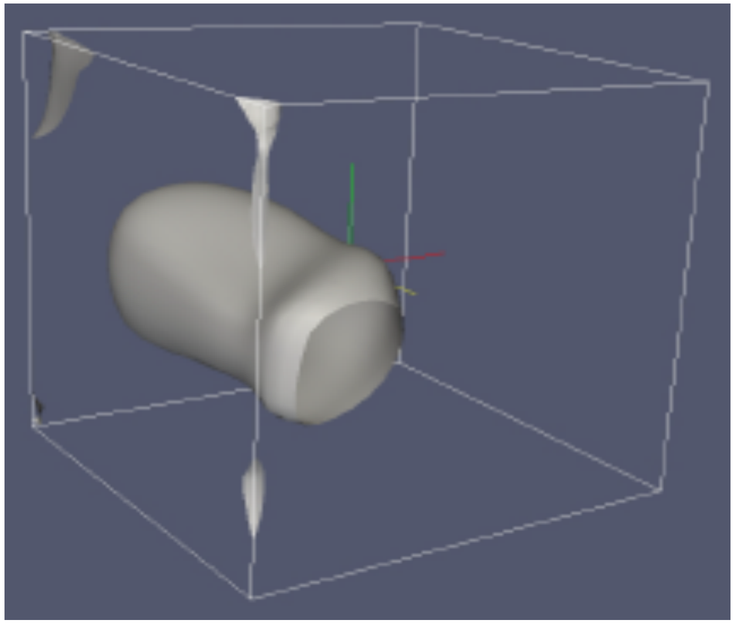

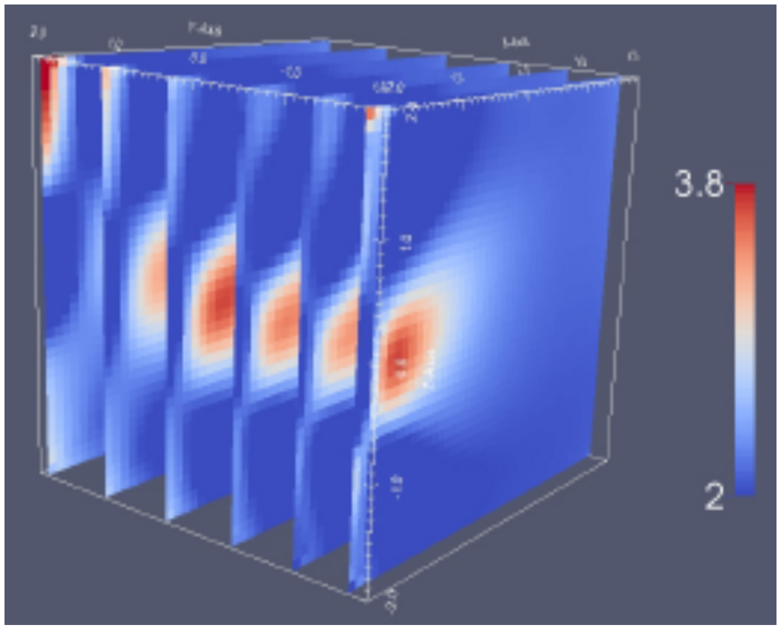

Simultaneously reconstruction of 2 coefficients

600 MHz, **3% of noise** **C = (4,0,0), D = 4 mm**

$g = 0.8$

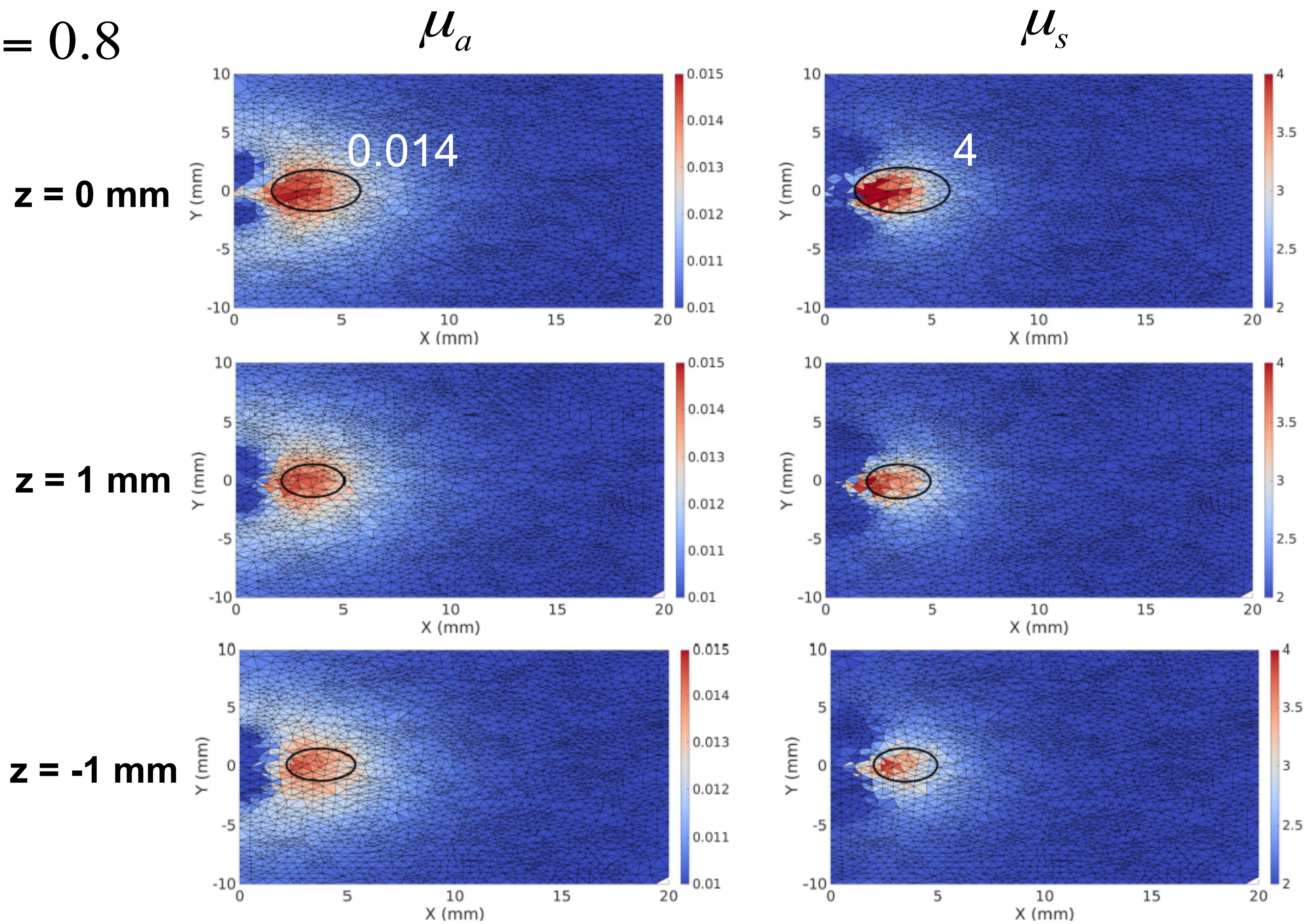

Challenge

• EXPLOR project, Nancy

• To test the reconstruction with a large amount of data: **1,5 million of nodes** (for the spatial mesh)

• Parallel computing (in frequency and direction) with MPI and Open MP, running on a set of multi-core machines (collab with LORIA Nancy)

- **256 directions**
- **8 frequencies** in [500 MHz, 1 GHz] (allows to be rich in information and to raise the under-determined character of the inverse problem)
- calculation during **1 week** (**21**/11 – **27**/11) on a cluster of **2048 cores**

Diagnosis with Fluorescence

Collab with

- Pr Kienle (Germany)
- Institut de Cancérologie de Lorraine

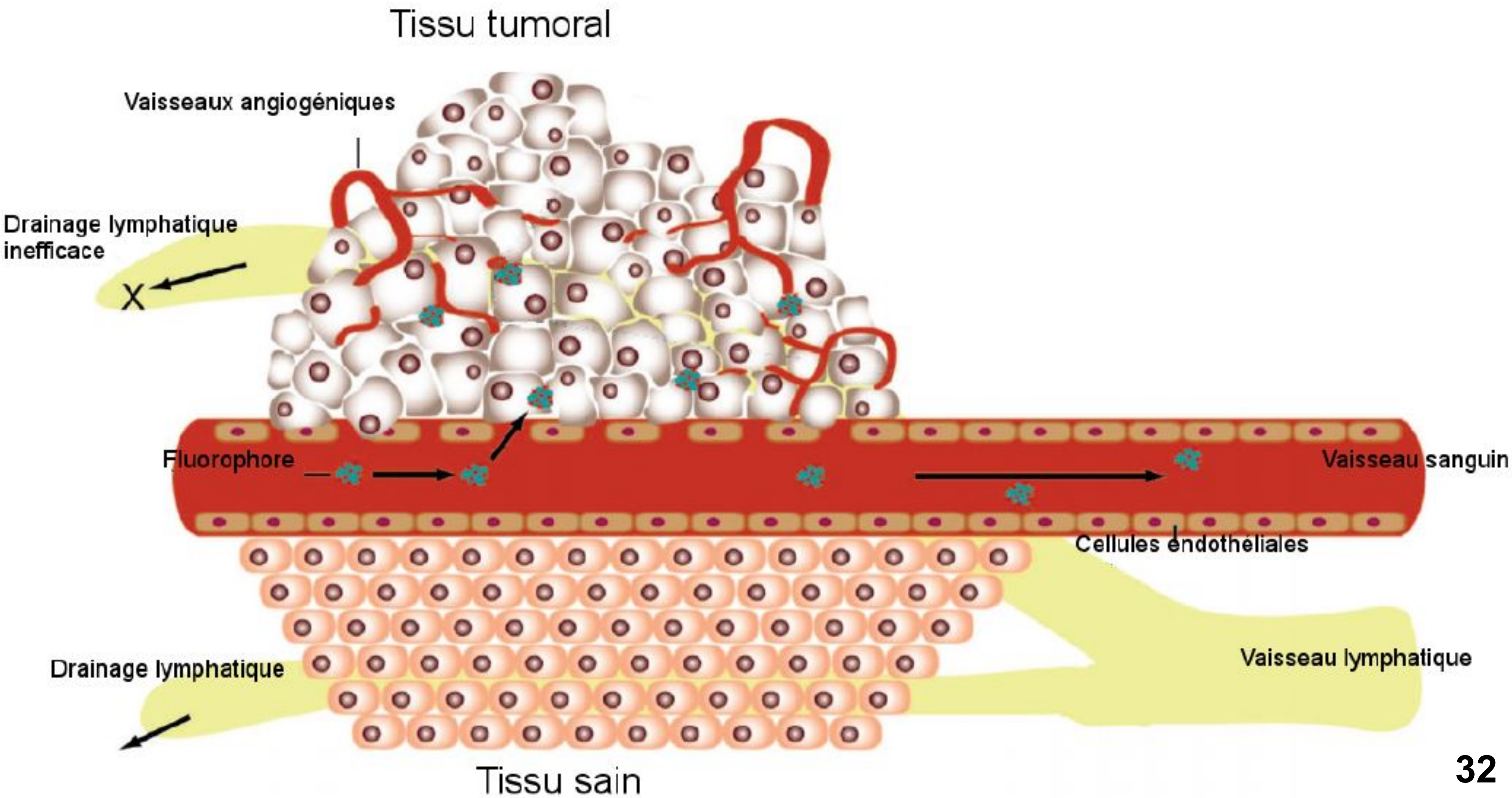

Diagnosis with Fluorescence

Collab with

- Pr Kienle (Germany)
- Institut de Cancérologie de Lorraine

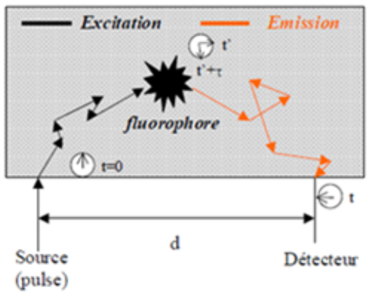

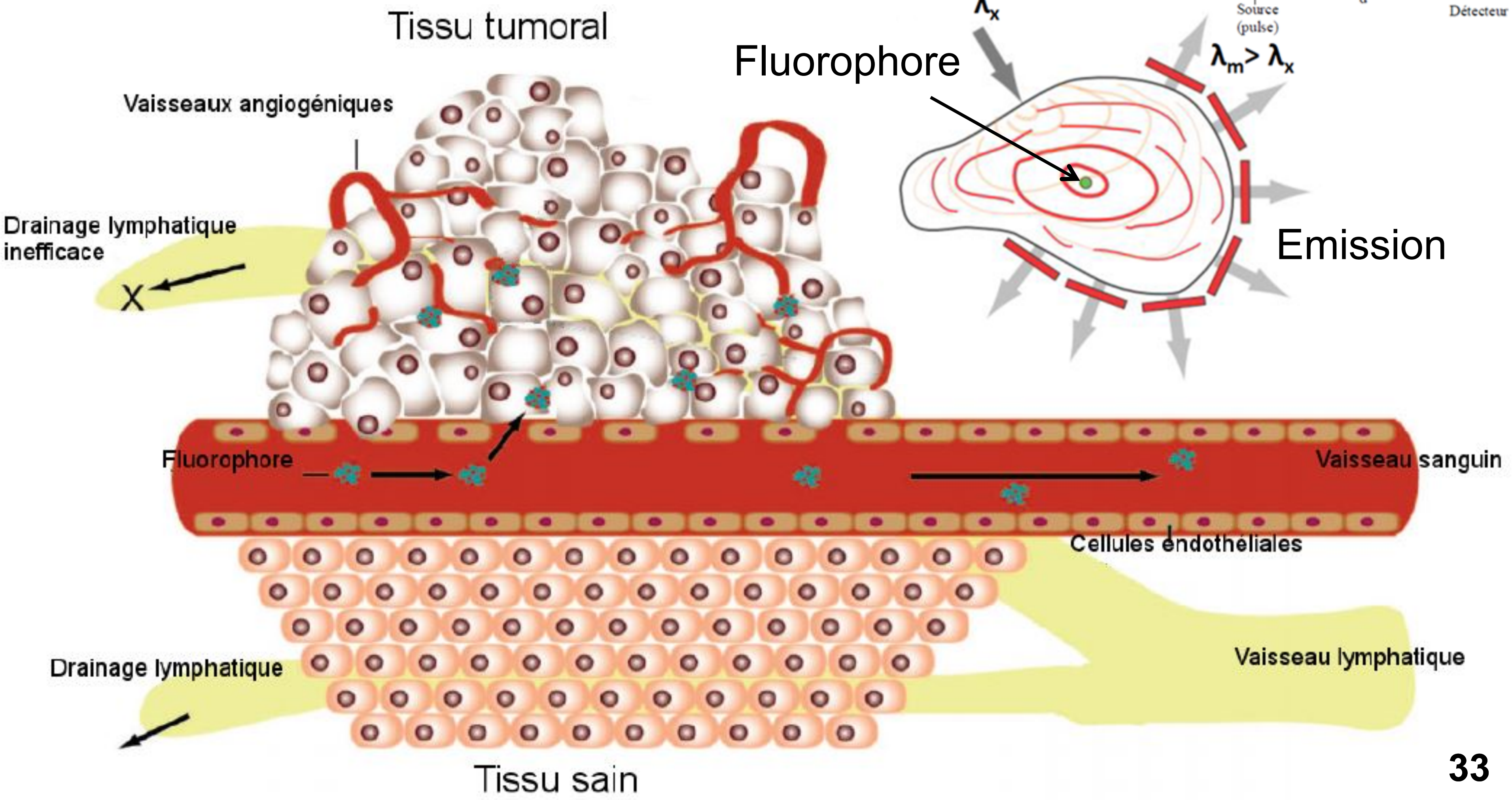

Fluorescence light model

- Excitation at λ^x

$$\left(\mathbf{\Omega}\cdot\nabla + \frac{i\omega_m}{v^x} + \mu_t^x(\boldsymbol{r}) + \mu_a^{x\to m}(\boldsymbol{r})\right)\psi^x(\boldsymbol{r},\mathbf{\Omega},\omega_m) = \mu_s^x(\boldsymbol{r})\int_{\Omega'=4\pi} p^x(\mathbf{\Omega}',\mathbf{\Omega})\,\psi^x(\boldsymbol{r},\mathbf{\Omega}',\omega_m)\,d\Omega'$$

- Emission at λ^m

$$\left(\mathbf{\Omega}\cdot\nabla + \frac{i\omega_m}{v^m} + \mu_t^m(\boldsymbol{r})\right)\psi^m(\boldsymbol{r},\mathbf{\Omega},\omega_m) = \mu_s^m(\boldsymbol{r})\int_{\Omega'=4\pi} p^m(\mathbf{\Omega}',\mathbf{\Omega})\,\psi^m(\boldsymbol{r},\mathbf{\Omega}',\omega_m)\,d\Omega'$$

$$+\frac{\eta(\boldsymbol{r})\ \mu_a^{x\to m}(\boldsymbol{r})}{1+i\,\omega_m\,\tau(\boldsymbol{r})}\int_{\Omega=4\pi}\psi^x(\boldsymbol{r},\mathbf{\Omega},\omega_m)\,d\Omega$$

Fluorescence light model

- Excitation at λ^x

= $\varepsilon\, C$ (= concentration)

$$\left(\mathbf{\Omega}\cdot\nabla + \frac{i\omega_m}{v^x} + \mu_t^x(\boldsymbol{r}) + \mu_a^{x\to m}(\boldsymbol{r})\right)\psi^x(\boldsymbol{r},\mathbf{\Omega},\omega_m) = \mu_s^x(\boldsymbol{r})\int_{\Omega'=4\pi} p^x(\mathbf{\Omega}',\mathbf{\Omega})\,\psi^x(\boldsymbol{r},\mathbf{\Omega}',\omega_m)\,d\Omega'$$

- Emission at λ^m

absorption coefficient of fluorophores

$$\left(\mathbf{\Omega}\cdot\nabla + \frac{i\omega_m}{v^m} + \mu_t^m(\boldsymbol{r})\right)\psi^m(\boldsymbol{r},\mathbf{\Omega},\omega_m) = \mu_s^m(\boldsymbol{r})\int_{\Omega'=4\pi} p^m(\mathbf{\Omega}',\mathbf{\Omega})\,\psi^m(\boldsymbol{r},\mathbf{\Omega}',\omega_m)\,d\Omega'$$

$$+\frac{\eta(\boldsymbol{r})\,\mu_a^{x\to m}(\boldsymbol{r})}{1+i\,\omega_m\,\tau(\boldsymbol{r})}\int_{\Omega=4\pi}\psi^x(\boldsymbol{r},\mathbf{\Omega},\omega_m)\,d\Omega$$

Fluorescence light model

- Excitation at λ^x

= $\varepsilon\, C$ (= concentration)

$$\left(\mathbf{\Omega}\cdot\nabla + \frac{i\omega_m}{v^x} + \mu_t^x(\boldsymbol{r}) + \mu_a^{x\to m}(\boldsymbol{r})\right)\psi^x(\boldsymbol{r},\mathbf{\Omega},\omega_m) = \mu_s^x(\boldsymbol{r})\int_{\Omega'=4\pi} p^x(\mathbf{\Omega'},\mathbf{\Omega})\,\psi^x(\boldsymbol{r},\mathbf{\Omega'},\omega_m)\,d\Omega'$$

- Emission at λ^m

absorption coefficient of fluorophores

$$\left(\mathbf{\Omega}\cdot\nabla + \frac{i\omega_m}{v^m} + \mu_t^m(\boldsymbol{r})\right)\psi^m(\boldsymbol{r},\mathbf{\Omega},\omega_m) = \mu_s^m(\boldsymbol{r})\int_{\Omega'=4\pi} p^m(\mathbf{\Omega'},\mathbf{\Omega})\,\psi^m(\boldsymbol{r},\mathbf{\Omega'},\omega_m)\,d\Omega'$$

$$+\frac{\eta(\boldsymbol{r})\,\mu_a^{x\to m}(\boldsymbol{r})}{1+i\,\omega_m\,\tau(\boldsymbol{r})}\int_{\Omega=4\pi}\psi^x(\boldsymbol{r},\mathbf{\Omega},\omega_m)\,d\Omega$$

- **Adjoint in fluorescence** (collab with a mathematician of Nancy)

Emission $\left(\mathbf{\Omega}\cdot\nabla - \frac{i\omega_m}{v^m} + \mu_t^m(\boldsymbol{r})\right)\phi^m(\boldsymbol{r},-\mathbf{\Omega},\omega_m) = \mu_s^m(\boldsymbol{r})\int_{\Omega'=4\pi} p^m(\mathbf{\Omega'},-\mathbf{\Omega})\,\phi^m(\boldsymbol{r},\mathbf{\Omega'},\omega_m)\,d\Omega'$

Diffuse excitation, $\phi_s^x(\boldsymbol{r},-\mathbf{\Omega},\omega_m)$ depending on ϕ^m

Collimated excitation, $\phi_c^x(\boldsymbol{r},\omega_m)$ depending on ϕ^m and ϕ_s^x

+ adjoint BC

Analytical expression of $\nabla J(\mu_a^{x\to m})$

2D reconstruction of the absorption of fluorophore

100 MHz $\mu_a^x = \mu_a^m = 0.1\,\mathrm{cm}^{-1}; \mu_s^x = \mu_s^m = 100\,\mathrm{cm}^{-1}; g^x = g^m = 0.9$

$\eta = 0.012;\ \tau = 0.52\ \mathrm{ns}$ (Indocyanine Green)

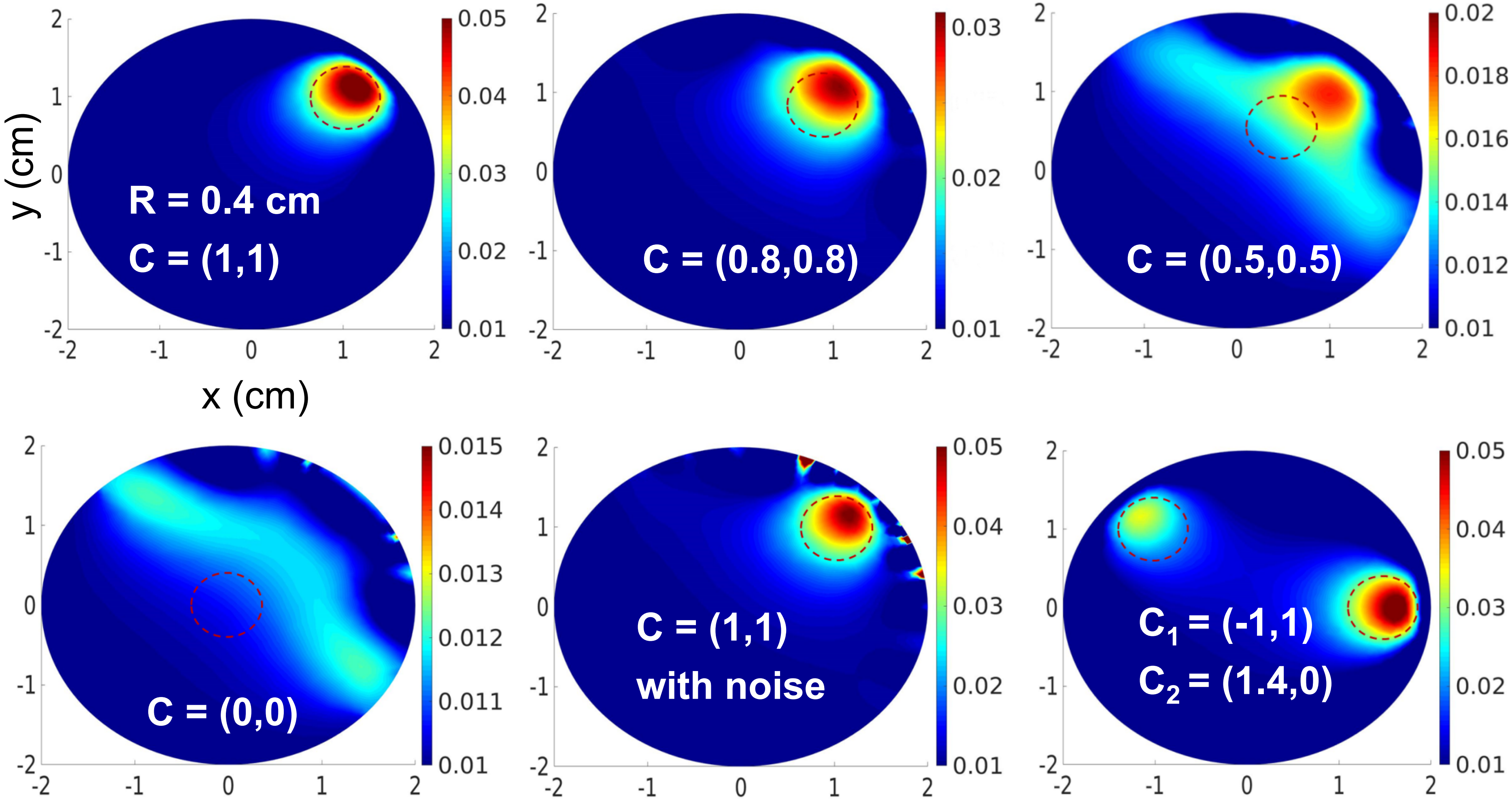

Asllanaj et al. (**2017,** submitted), **Inverse Problems**

Conclusions on the MFVM

- **Advantages**

- Suitable for predicting fluorescence and diffuse light propagation in absorbing and highly forward-scattering media subjected to a collimated laser beam

- Good level of accuracy; a relative difference < 1% can be obtained when compared to MC or analytical solutions

- Explicit solution of the radiance (without solving a linear system)

- Use of unstructured meshes

Conclusions on the MFVM

- **Advantages**

- Suitable for predicting fluorescence and diffuse light propagation in absorbing and highly forward-scattering media subjected to a collimated laser beam

- Good level of accuracy; a relative difference < 1% can be obtained when compared to MC or analytical solutions

- Explicit solution of the radiance (without solving a linear system)

- Use of unstructured meshes

- **(Actual) disadvantage:** time consuming

- 256 (or more) RTEs have to be solved (in the multiple scattering regime). Several iterations (100 - 1000) are needed to compute the different orders of scattering

Conclusions on the optical tomography software

• Based on an accurate deterministic forward model

• Can reconstruct (in 2D/3D):

- $\mu_a(\boldsymbol{r}), \mu_s(\boldsymbol{r}), g(\boldsymbol{r})$

  Actually, 2 coefficients can be reconstructed simultaneously but not 3

- $\mu_a^{x \to m}(\boldsymbol{r})$

• The 3D computational times are actually too high for a (pre)clinical application

• Probably, we can optimize the MVFM and the inverse algorithm..., couple MVFM and MC, ...

Future works

- **Optical imaging**

- **Applications**:

  - Validation on (epoxy resin) phantoms (with Pr Kienle, Germany)

  - **Project** with the **Institut de Cancérologie de Lorraine** on the study of fluorophore diffusion (used in **Photodynamic Therapy**) in a preclinical model (multicellular tumor spheroid model)

Future works

- **Optical imaging**
- **Applications**:

  \- Validation on (epoxy resin) phantoms (with Pr Kienle, Germany)

  \- **Project** with the **Institut de Cancérologie de Lorraine** on the study of fluorophore diffusion (used in **Photodynamic Therapy**) in a preclinical model (multicellular tumor spheroid model)

- **Photoacoustic imaging** (take advantage of optic and acoustic for a high spatial resolution and a deeper penetration)

Future works

- **Optical imaging**
- **Applications**:

  - Validation on (epoxy resin) phantoms (with Pr Kienle, Germany)

  - **Project** with the **Institut de Cancérologie de Lorraine** on the study of fluorophore diffusion (used in **Photodynamic Therapy**) in a preclinical model (multicellular tumor spheroid model)

- **Photoacoustic imaging** (take advantage of optic and acoustic for a high spatial resolution and a deeper penetration)
- **Coupled heat transfers in biological tissues:** study of the tissue denaturation mechanism

Thank you for your attention!

Collaborations

Pr Contassot-Vivier

Loria

Laboratoire lorrain de recherche en informatique et ses applications

Pr Kienle

Institut for **L**aser Technology in **M**edicine and Metrology

ulm university universität ulm

Angewandte Photonik **(stay of 10 months)**

Pr J. R. Roche

Institute of Mathematics, Lorraine

Institut ÉLIE CARTAN

Pr L. Bolotine

S. Marchal, CR

Institut de Cancérologie de Lorraine

Alexis Vautrin

Ensemble, construisons l'avenir

Semitransparent boundaries

- Specular reflection

$$\psi(s,\boldsymbol{\Omega},t) \;=\; \big(1-\rho(\Theta)\big)\,\Upsilon(s,\boldsymbol{\Omega},t) \;+\; \rho(\Theta)\,\psi(s,\boldsymbol{\Omega_{inc}},t) \quad \text{for} \quad \boldsymbol{\Omega}\cdot\boldsymbol{n} > 0,$$

where $\boldsymbol{\Omega}$ is the specular reflection of $\boldsymbol{\Omega_{inc}}$: $\boldsymbol{\Omega_{inc}} = \boldsymbol{\Omega} - 2\,(\boldsymbol{\Omega}\cdot\boldsymbol{n})\,\boldsymbol{n}$. The angle Θ satisfies $\cos\Theta = \boldsymbol{\Omega_{inc}}\cdot\boldsymbol{n_{out}} > 0$ where $\boldsymbol{n_{out}}$ is local unit outward normal vector. The directional reflection $\rho(\Theta)$ is given by Snell-Descartes laws. Considering that $n^2 \ll k^2$ (n, k being the real and imaginary parts of the complex refractive index, respectively):

$$\rho(\Theta) \;=\; \begin{cases} \frac{1}{2}\left(\frac{\cos\Theta - n_r R(\Theta)}{\cos\Theta + n_r R(\Theta)}\right)^2 + \frac{1}{2}\left(\frac{n_r\cos\Theta - R(\Theta)}{n_r\cos\Theta + R(\Theta)}\right)^2 & \text{if} \quad \Theta < \Theta_{crit} \\ 1 & \text{otherwise,} \end{cases}$$

with $R(\Theta) = \sqrt{1 - n_r^2\sin^2\Theta}$ and $n_r = \frac{n}{n_{out}}$ is the relative refractive index between the two media. The critical angle satisfies Snell's law: $\sin\Theta_{crit} = n_r^{-1}$. In our application, $n_{out} = 1$, $n_r = n = 1.4$ and $\Theta_{crit} = 45.58^{o}$.

- Diffuse reflection

Change $\rho(\Theta)\,\psi(s,\boldsymbol{\Omega}_{\text{inc}},t)$ by $\dfrac{1}{\pi}Q_{out}(s,t)$

Biomedical diagnosis

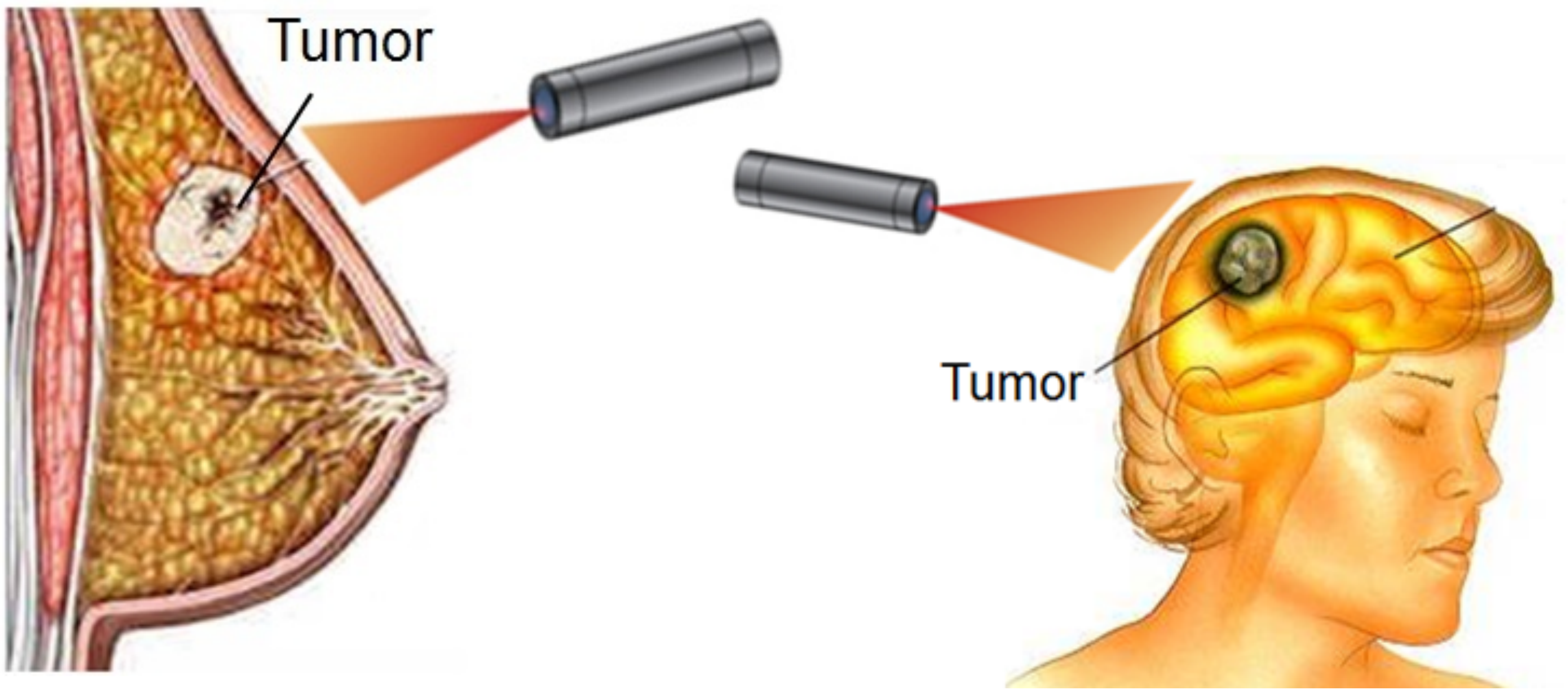

- **An important issue in Optical Tomography** is to have an **efficient forward solver** (accurate, fast, suitable for irregular geometries) combined with an **efficient inverse method** for reconstructing the mesoscopic optical properties

Different methods for solving the RTE

Diffusion Equation

- Approximate model (deduced from the RTE) yet widely used

- 3 assumptions:

(1) low absorption, $\mu_a << \mu_s$

(2) large spatial and time scales, $l_{tr} << L$ and $\dfrac{l_{tr}}{c} << T$

$l_{tr} = 1/\mu_s^*$: transport length with $\mu_s^* = \mu_s\,(1-g)$

= path taken by a collimated beam before it becomes isotropic

T: observation time. *L*: characteristic length of the medium

(3) does not correctly model the BC with a collimated (laser) beam

Reconstruction of μs

600 MHz

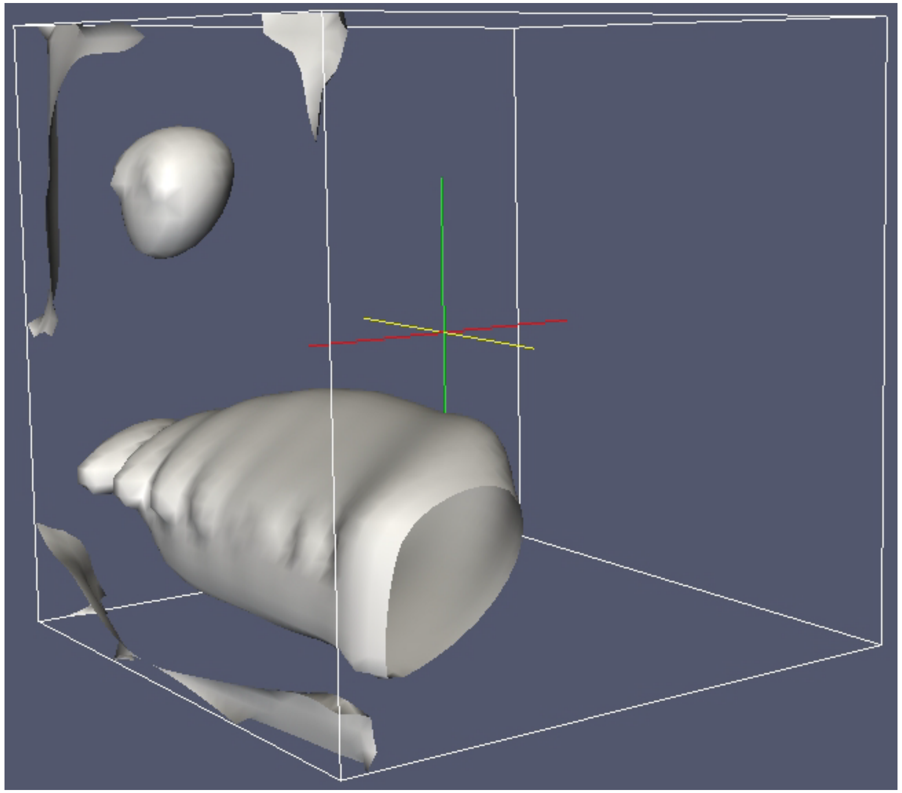

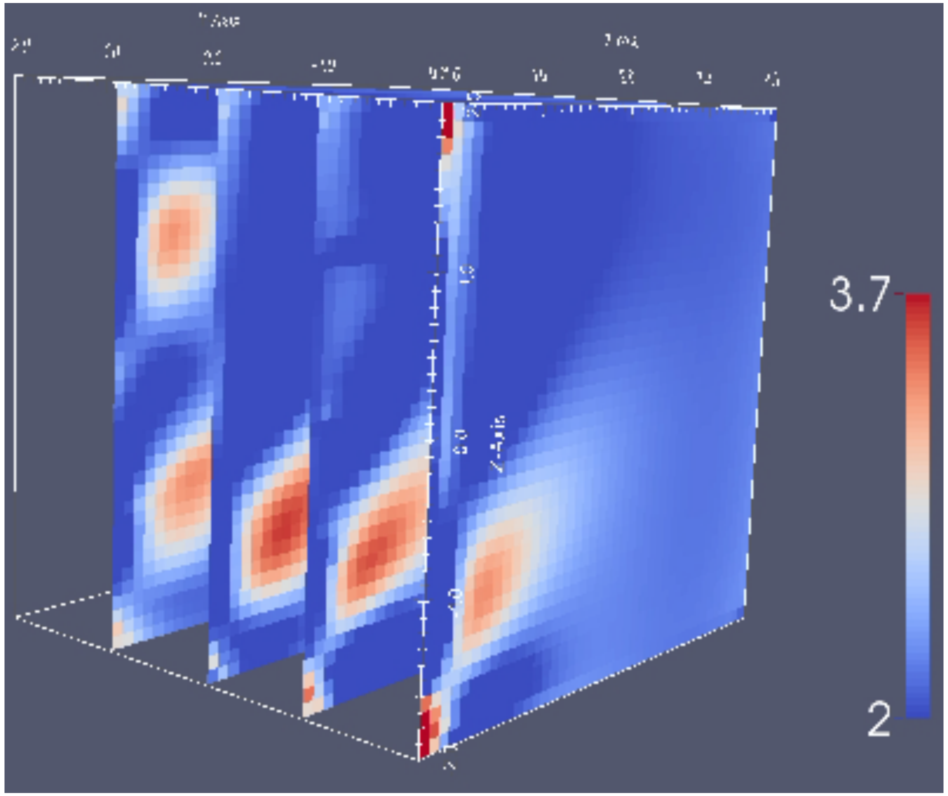

3D

Perpendicular incident beam

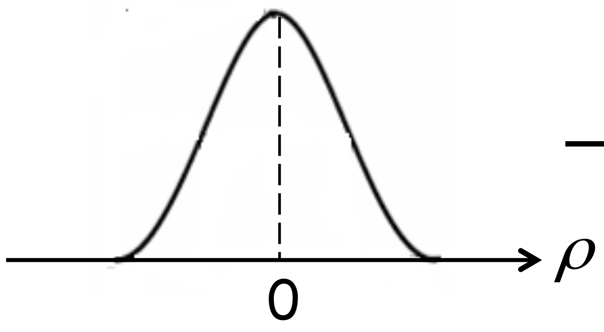

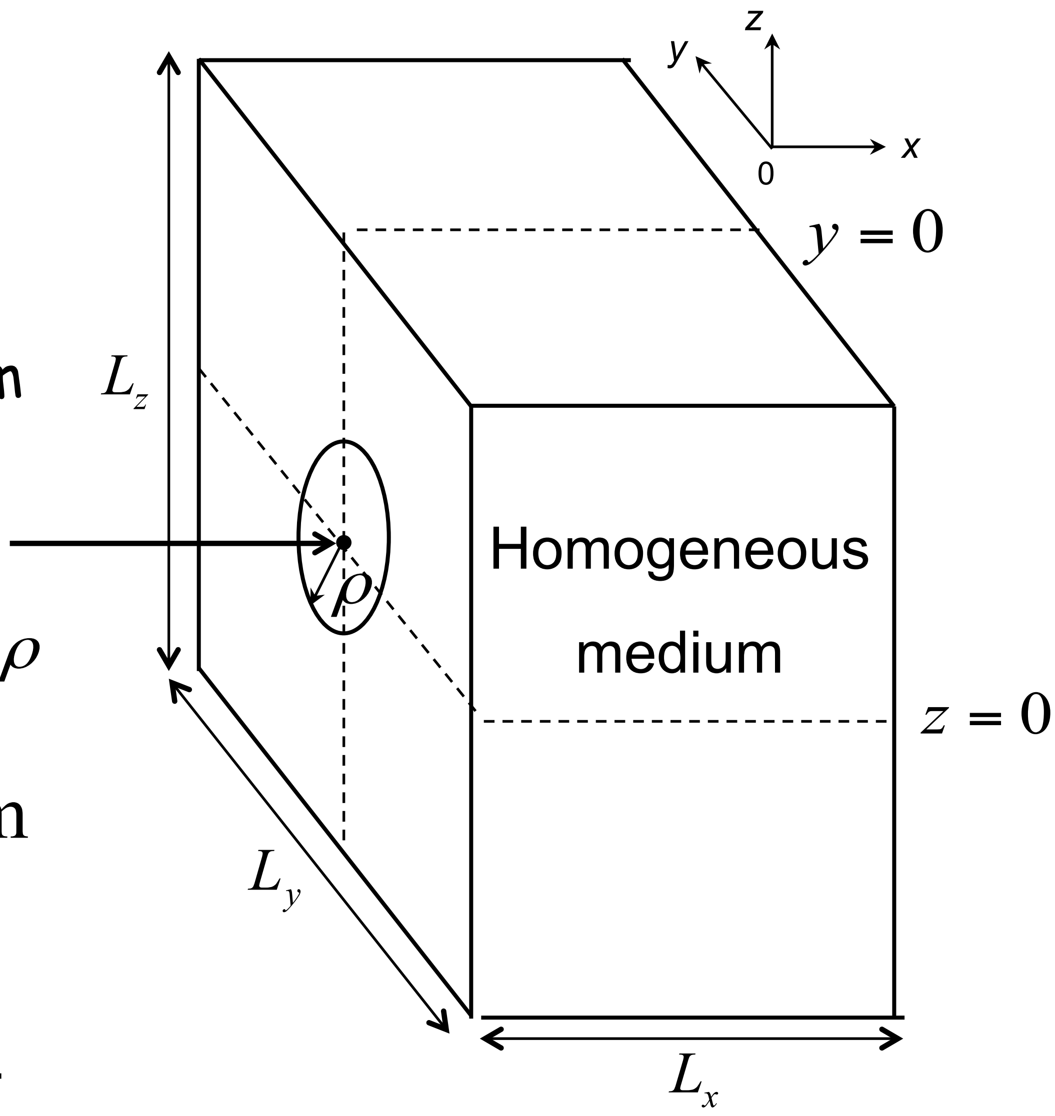

$$L_y = L_z = 12\ \mathrm{mm}$$

$$L_x = 10\ \mathrm{mm}$$

$$n_{air} = 1\ ;\ n = 1.4$$

Semi-transparent boundaries

Elastically scattered light

- Incident beam

$$S(\rho) = \frac{2}{\pi\,\varepsilon^2}\exp\left(-\frac{2\rho^2}{\varepsilon^2}\right)$$

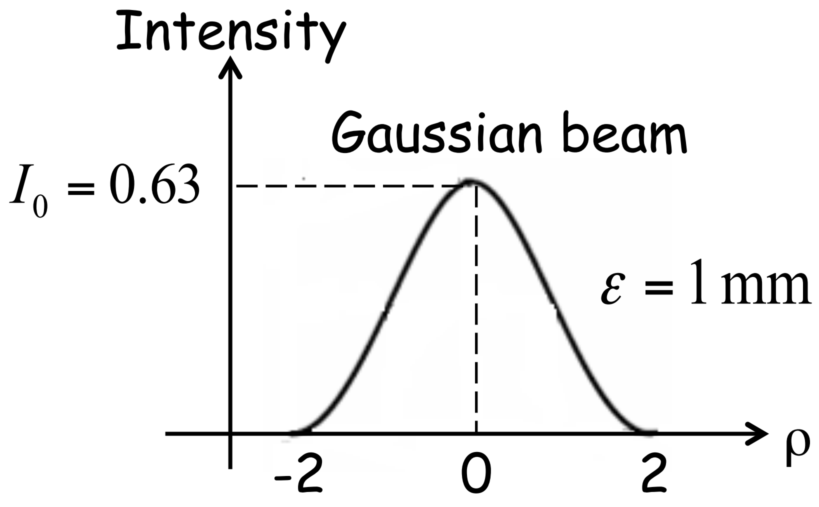

The spatial mesh (in the plane (Oyz)) was refined around the strong variation of the Gaussian function

1st case

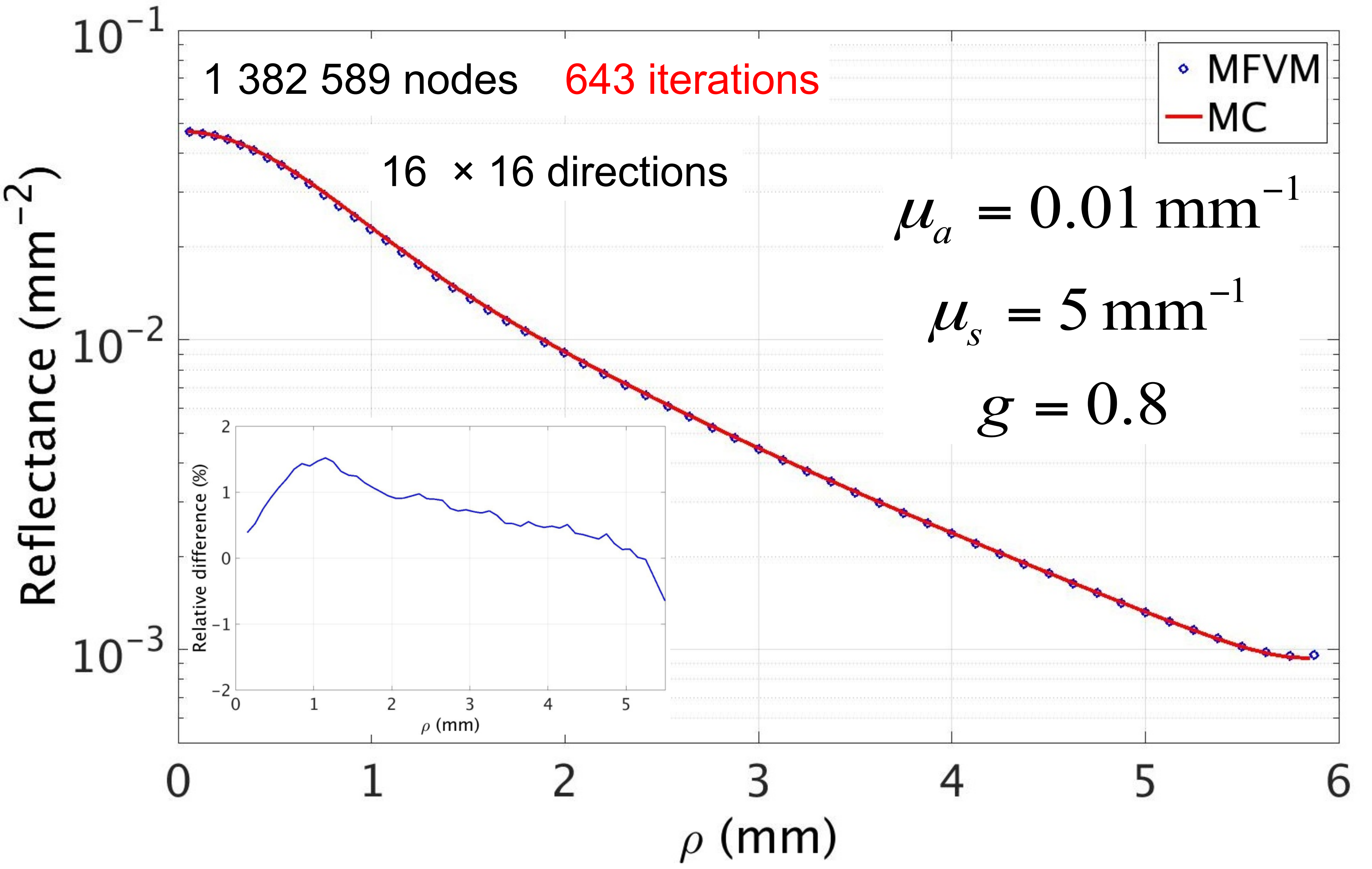

1 382 589 nodes
643 iterations
16 × 16 directions
MFVM
MC
$\mu_a = 0.01\ \mathrm{mm}^{-1}$
$\mu_s = 5\ \mathrm{mm}^{-1}$
$g = 0.8$
Reflectance (mm^{-2})
10^{-1}
10^{-2}
10^{-3}
0
1
2
3
4
5
6
ρ (mm)
Relative difference (%)
2
1
0
−1
−2
0
1
2
3
4
5
ρ (mm)

2^{nd} case

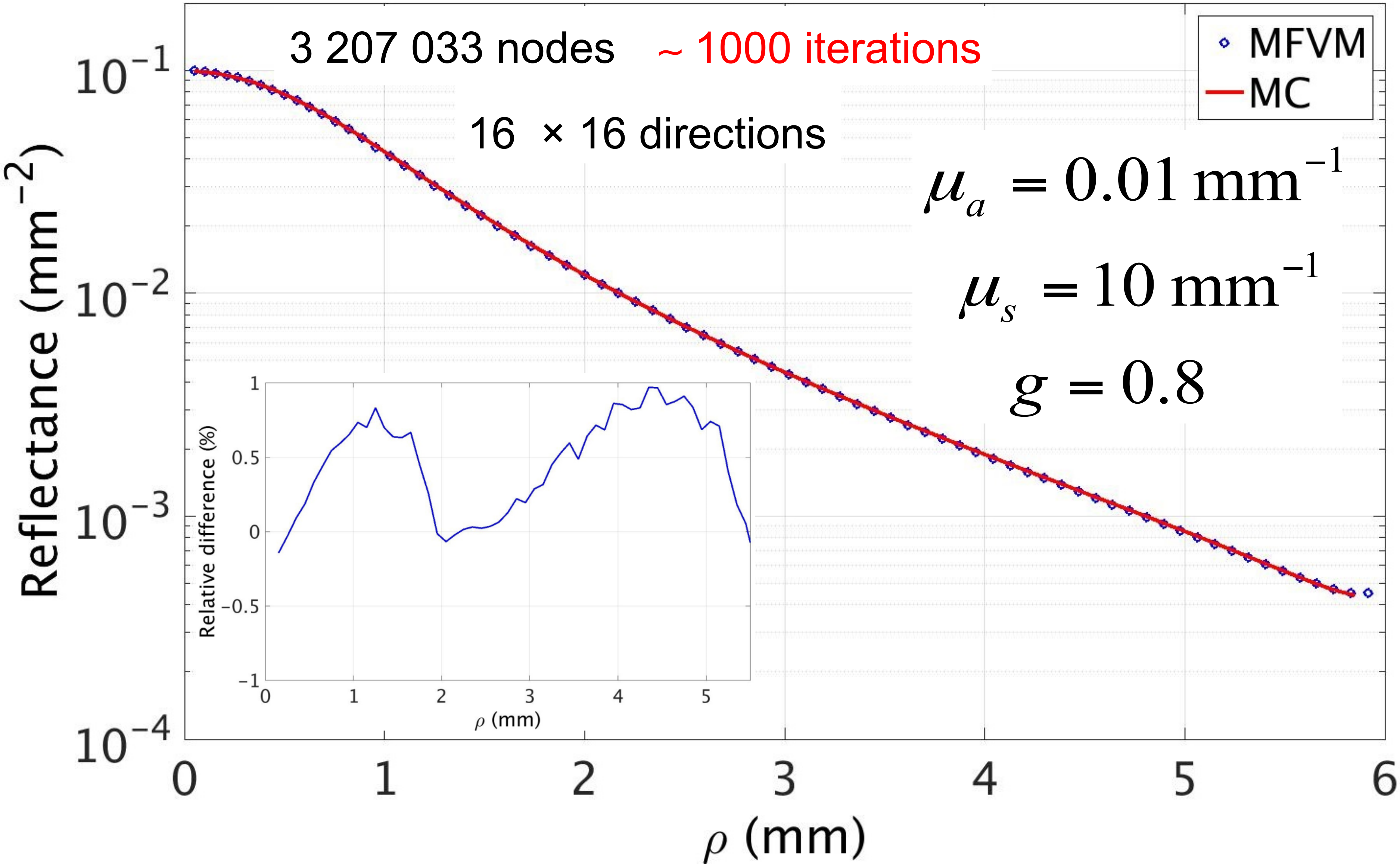

3 207 033 nodes
~ 1000 iterations
16 × 16 directions
$\mu_a = 0.01 \text{ mm}^{-1}$
$\mu_s = 10 \text{ mm}^{-1}$
$g = 0.8$
MFVM
MC
Reflectance (mm^{-2})
ρ (mm)
Relative difference (%)
ρ (mm)

3rd case

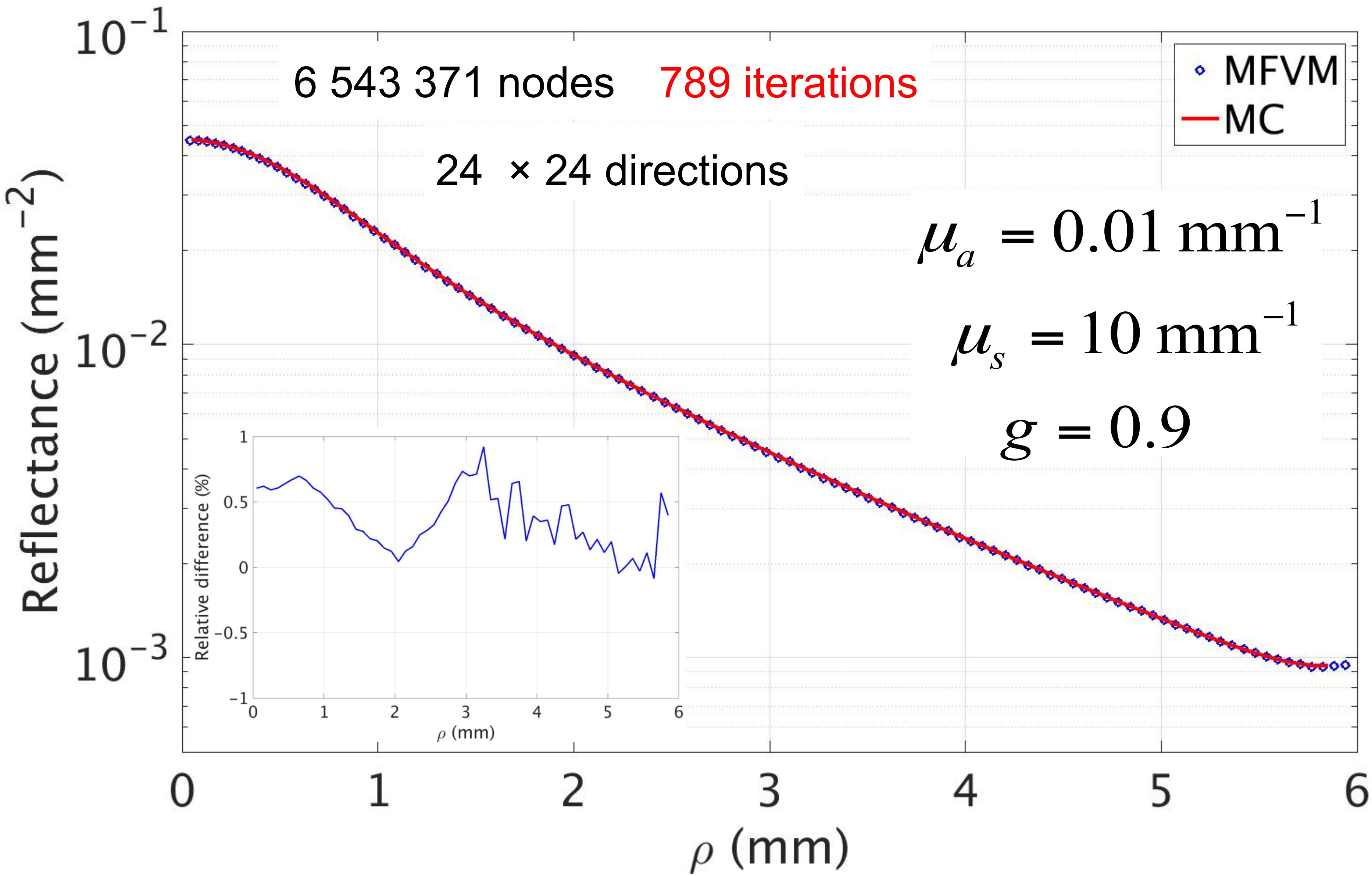
6 543 371 nodes
789 iterations
24 × 24 directions
$\mu_a = 0.01\ \mathrm{mm}^{-1}$
$\mu_s = 10\ \mathrm{mm}^{-1}$
$g = 0.9$
MFVM
MC
Reflectance (mm^{-2})
ρ (mm)
10^{-1}
10^{-2}
10^{-3}
0
1
2
3
4
5
6
Relative difference (%)
1
0.5
0
−0.5
−1